CRAFT: Corpus Relatedness Analysis Using Fourier Transforms

Kaiwen Chen
University Of Toronto
Toronto, Ontario, Canada
kckevinchen@cs.toronto.edu

Nick Koudas
University Of Toronto
Toronto, Ontario, Canada
koudas@cs.toronto.edu

Abstract

A fundamental challenge in data management is the efficient discovery of term relationships from massive, unstructured text corpora, a critical first step in knowledge graph construction. This discovery task, however, faces prohibitive computational barriers: the quadratic $O(N^2)$ complexity of an all-pairs analysis and the intractability of processing the full term-document matrix. While dimensionality reduction via embeddings offers a partial solution, the resulting vector proximity often captures broad thematic similarity, failing to isolate the precise co-occurrence signals required for high-quality relation extraction.

This paper introduces CRAFT, a system that overcomes these limitations by re-casting term relatedness discovery as a scalable signal processing problem. CRAFT's methodology decouples the discovery process from both the term-document matrix and quadratic-time comparisons. First, it employs a randomized Fourier transform to sketch term occurrence signals directly into a low dimensional complex space, a process that provably preserves the inner products essential for correlation analysis without materializing the underlying matrix. Second, to break the quadratic barrier, CRAFT leverages the inherent sparsity of term relationships by formulating discovery as a compressed sensing task. This enables the recovery of significant correlations for any given term directly from its compressed sketch via an efficient Orthogonal Matching Pursuit algorithm, obviating the need for an all-pairs comparison. Our end-to-end implementation and comprehensive experimental evaluation show that CRAFT significantly outperforms modern baselines in both efficiency and precision, enabling high-quality relation discovery at a previously infeasible scale.

1 Introduction

Identifying frequently co-occurring terms in massive, unstructured text corpora is fundamental to modern data management and AI. When terms consistently appear together—what we call relatedness—they exhibit strong semantic or functional associations arising from shared topics ((e.g., "iPhone" and "Apple"), common contexts (e.g., "aspirin" and "blood clot" in medicine), or compound concepts (e.g., "machine learning"). This capability is critical for applications ranging from query expansion and trend analysis to knowledge discovery in scientific literature [10, 17, 44]. A primary application is constructing Knowledge Graphs (KGs) in novel domains [2, 4, 22]. KGs represent information as networks of entities and relationships, powering semantic search and question-answering systems. They are increasingly vital for grounding Large Language Models (LLMs) [33, 37, 38], serving as verifiable memory sources in Retrieval-Augmented Generation (RAG) [28] frameworks to reduce hallucinations and inject domain-specific facts. However, their utility is constrained by a fundamental computational bottleneck: bootstrapping the graph from raw, unstructured text. This bottleneck centers on the candidate discovery problem: scalably identifying potentially related terms before fine-grained analysis. Current academic benchmarks [7, 36] largely sidestep this challenge, focusing instead on relation classification—assigning semantic labels to pre-identified entity pairs [27, 35]. This assumes a domain-adapted Entity Recognition tool has already identified all relevant entities, effectively bypassing the core challenge: one cannot leverage a domain-specific KG without first constructing it from source text. In real-world scenarios with novel, domain-specific corpora (scientific literature, financial reports, enterprise documents), this assumption fails. The task becomes a massive-scale filtering problem: evaluating the combinatorially vast space of potential term pairs—scaling quadratically $O(N^2)$ with vocabulary size N—to isolate the tiny fraction that are meaningfully related.

Existing methods make critical trade-offs. Brute-force pairwise analysis (e.g., Pointwise Mutual Information [11], co-occurrence graphs) generates massive noise and impractically dense outputs. Embedding-based methods [34, 39, 47] are designed to capture semantic similarity—mapping terms with similar meanings (e.g., 'physician' and 'doctor') to nearby points in vector space. However, this does not imply rigorous statistical correlation. This limitation stems from the distinction between paradigmatic and syntagmatic relationships. Embedding methods primarily capture paradigmatic similarity—terms that can substitute for one another in a sentence (e.g., 'physician' and 'doctor'). However, knowledge discovery often requires identifying syntagmatic associations—terms that physically co-occur to form a functional unit (e.g., 'physician' and 'prescription'). CRAFT is explicitly designed to isolate these syntagmatic signals via correlation analysis. Our empirical evaluation explicitly validates this distinction in Section 6.4.5. LLMs excel at focused reasoning but cannot perform exhaustive corpus-wide discovery and are prone to hallucinating unsupported relationships [23]. This gap demands a scalable "first-pass" filter for candidate discovery, one that complements LLMs in a hybrid approach: lightweight discovery at scale, followed by economical LLM-based verification using corpus evidence. We introduce **CRAFT** (Corpus Relatedness Analysis Using Fourier Transforms), a novel paradigm addressing this exact need, as shown in Figure 1. We distinguish between inferring latent similarity and measuring observable correlation. CRAFT is designed strictly for the latter. Rather than learning opaque dense vectors, CRAFT treats term presence as discrete signals and processes them in compact frequency representations to identify persistent co-occurrences with remarkable efficiency, formally relating co-occurrence to statistical correlations (Pearson's coefficient). This produces a clean, high-precision candidate set ideal for KG bootstrapping, search enrichment, or LLM validation. Our key insight: the sparsity-of-effects principle—most terms interact significantly with only a small number of others.
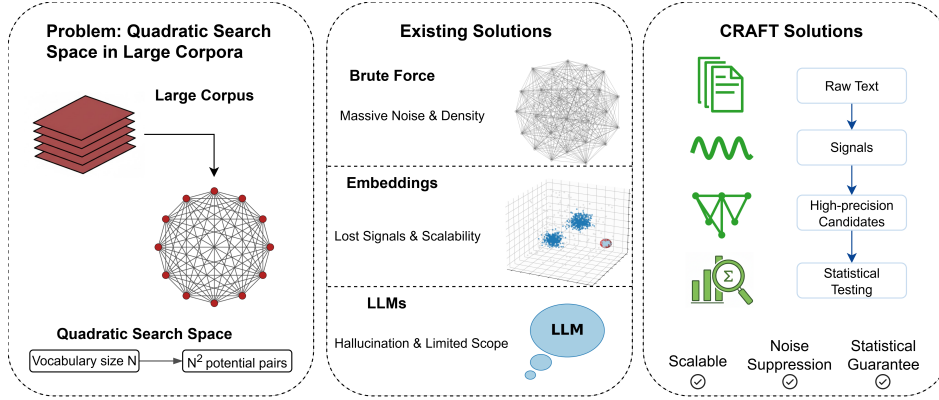
Figure 1: The CRAFT paradigm. We overcome the $O(N^2)$ bottleneck of term discovery by treating it as a signal processing task, leveraging frequency-domain analysis to scalably identify meaningful relationships without exhaustive pairwise comparison.

The primary contributions of our work are as follows:[1]

- A Novel Signal Processing Paradigm for Text Analysis: We introduce CRAFT, a framework that reinterprets the problem of term relatedness discovery in large text corpora as a signal processing task. By treating the presence of terms across documents as discrete signals and analyzing their frequency-domain representations, CRAFT enables highly efficient and scalable detection of semantic relationships without relying on pre-existing knowledge bases or expensive pairwise computations.

- Randomized Fourier Embedding with Theoretical Guarantees: We propose a Random Fourier Transform (RFT)-based dimensionality reduction technique that projects high dimensional term vectors into a low dimensional complex space. This method preserves inner products with high probability, reducing storage and computation from $O(N^2M)$ to $O(Nk \log M)$ with $k \leq N$ (for N terms and M documents).

- Cross-Power Spectral Density (CPSD) for Correlation Estimation: We adapt Cross-Power Spectral Density (CPSD)—a classical signal processing tool—to estimate term statistical correlations in the frequency domain. CPSD not only captures the magnitude of correlation but also leverages phase information to distinguish between positive, negative, and orthogonal relationships, providing a richer and more interpretable measure of term association.

- Sparse Recovery via Compressed Sensing: We reformulate correlation recovery as a compressed sensing problem, leveraging the insight that most term relationships are sparse. We employ **Orthogonal Matching Pursuit (OMP)** [45], a computationally efficient algorithm, to recover sparse correlation vectors directly from their compressed measurements. This approach enables the identification of significant term pairs while completely avoiding the prohibitive cost of computing all $O(N^2)$ correlations.

- End-to-End Scalable System with Statistical Rigor: The full CRAFT pipeline integrates preprocessing, spectral sketching, CPSD-based correlation analysis, and sparse recovery into a cohesive system. We provide non-asymptotic error bounds, statistical significance testing with FDR control, and complexity guarantees, making the approach both practical and theoretically sound for real-world corpus-scale analysis.

- Empirical and Theoretical Superiority: We demonstrate through complexity analysis and empirical validation that CRAFT significantly outperforms existing methods in both speed and precision, enabling the discovery of high-quality relational candidates at a scale previously infeasible with state-of-the-art techniques.

2 Problem Formulation

Our goal is to automatically discover meaningful associations between terms by inductively analyzing a massive collection of unstructured text, such as a decade of biomedical preprints from arXiv's q-bio section or a proprietary repository of clinical trial documents from a pharmaceutical company. Unlike methods that rely on pre-existing ontologies, this approach processes the entire corpus—examining relatedness (co-occurrence) patterns across term pairs—to uncover significant statistical relationships without prior guidance on what to search for.

The aim is to generate a ranked list of strongly associated term pairs, such as (CRISPR, Cas9, 0.98) or (ibuprofen, cyclooxygenase, 0.92), where the numerical score reflects the strength of the relationship, the Pearson correlation coefficient. This method is especially powerful for revealing non-obvious yet plausible connections—for instance, linking metabolic pathways like *succinate* signaling to immune receptors such as *GPR91*, or associating *autophagy*-related genes like *ULK1* with specific cellular processes—effectively building the foundations of a novel knowledge graph directly from raw text. More formally our problem is defined as follows:

- **Input:** A corpus of documents $\mathcal{D} = \{d_1, d_2, \ldots, d_M\}$ and an associated vocabulary of terms $\mathcal{V} = \{w_1, w_2, \ldots, w_N\}$,

---

[1]Full report available at: https://github.com/kckevinchen/CRAFT

where N is the vocabulary size. V is typically derived by tokenizing C.

- **Output:** A ranked list of term pairs $\ell = [(v_i, v_j, s_{ij}), \dots]$, where (v_i, v_j) is a pair of distinct terms from V and $s_{ij} \in \mathbb{R}$ is a score representing the strength of their relationship expressed in terms of the Pearson correlation coefficient. The list is ordered by s_{ij} in descending order.

The objective is to generate this list ℓ in a computationally efficient and scalable manner. The methodology for evaluating the overall quality of the generated list ℓ, will be detailed in the experiments section.

3 Large-Scale Term Correlation Detection via Randomized Nonlinear Embedding and Spectral Analysis

This section details our methodology for efficiently detecting statistically significant correlations between all pairs of terms in a large corpus. We first formalize the problem using a term-document matrix, then describe a randomized dimensionality reduction technique with theoretical guarantees, and finally present our algorithms for correlation estimation, sparse recovery, and significance testing. All proofs of theorems and lemmas are omitted due to space constraints and are available in our technical report [1].

3.1 Term-Document Matrix Construction and Statistical Formulation

We represent the corpus as a term-document matrix $\mathbf{A} \in \mathbb{R}^{N \times M}$, where each element a_{ij} quantifies the importance of term w_i in document d_j. We employ the BM25 weighting function[42] [2], a state-of-the-art ranking function robust to document length variation:

$$a_{ij} = \frac{\text{tf}(w_i, d_j) \cdot (k_1 + 1)}{\text{tf}(w_i, d_j) + k_1 \cdot \left(1 - b + b \cdot \frac{|d_j|}{\text{avgdl}}\right)} \cdot \log\left(\frac{M + 1}{\text{df}(w_i) + 0.5}\right) \quad (1)$$

where $\text{tf}(w_i, d_j)$ is the term frequency of w_i in d_j, $|d_j|$ is the length of document d_j, avgdl is the average document length in $\mathcal{D}$, $\text{df}(w_i)$ is the document frequency of w_i, and $k_1 = 1.2$, $b = 0.75$ are standard tuning parameters.

To analyze correlation, we center each row of $\mathbf{A}$ to obtain a matrix of deviation vectors, $\tilde{\mathbf{A}}$. The centered value $\tilde{a}_{ij}$ for term w_i in document d_j is given by $\tilde{a}_{ij} = a_{ij} - \mu_i$, where $\mu_i = \frac{1}{M} \sum_{m=1}^{M} a_{im}$ is the mean score for term w_i. The Pearson correlation coefficient ρ_{ij} between terms w_i and w_j is then defined as the cosine similarity between their centered vectors $\tilde{\mathbf{a}}_i$ and $\tilde{\mathbf{a}}_j$:

$$\rho_{ij} = \frac{\langle \tilde{\mathbf{a}}_i, \tilde{\mathbf{a}}_j \rangle}{\|\tilde{\mathbf{a}}_i\|_2 \|\tilde{\mathbf{a}}_j\|_2} = \frac{\sum_{m=1}^{M} \tilde{a}_{im} \tilde{a}_{jm}}{\sqrt{\sum_{m=1}^{M} \tilde{a}_{im}^2} \sqrt{\sum_{m=1}^{M} \tilde{a}_{jm}^2}} \quad (2)$$

The direct computation of the full $N \times N$ correlation matrix requires $O(N^2 M)$ operations and $O(NM)$ storage, which is computationally infeasible for large N and M.

---

[2] Any weighting function from the literature will work.

3.2 Randomized Fourier Embedding with Energy Preservation Guarantees

To overcome this limitation, we employ a randomized nonlinear embedding based on the method of Random Fourier Features (RFF) [40]. We project the high-dimensional, centered term vectors $\tilde{\mathbf{a}}_i$ into a significantly lower-dimensional complex space $\mathbb{C}^k$ while *provably preserving* the inner product information between vectors.

Formally, for each centered term vector $\tilde{\mathbf{a}}_i \in \mathbb{R}^M$, we compute its low-dimensional complex representation $\mathbf{b}_i \in \mathbb{C}^k$ via the following linear transformation:

$$\mathbf{b}_i = \frac{1}{\sqrt{k}} \Phi \tilde{\mathbf{a}}_i \quad (3)$$

The crucial element of this embedding is the *random Fourier matrix* $\Phi \in \mathbb{C}^{K \times M}$. The entries of Φ are not learned from data but are generated stochastically. Each element is defined by:

$$\phi_{lm} = e^{-2\pi i \xi_l m / M} \quad \text{for} \quad l = 1, \dots, k \quad \text{and} \quad m = 1, \dots, M, \quad (4)$$

where each frequency parameter ξ_l is sampled independently and identically from a Uniform$(0, 1)$ distribution.

Theoretical Underpinnings and Guarantees. This approach is grounded in Bochner's Theorem [30], which states that any continuous, shift-invariant kernel function (e.g., Gaussian Kernel) is the Fourier transform of a unique non-negative measure. The inner product $\mathbf{b}_i^* \mathbf{b}_j$ in the embedded space (where $\mathbf{b}_i^*$ denotes conjugate transpose) is an unbiased estimator of a shift-invariant kernel evaluation $K(\tilde{\mathbf{a}}_i, \tilde{\mathbf{a}}_j)$ in the original space. For our specific construction, this kernel is the linear kernel, $K(\mathbf{x}, \mathbf{y}) = \mathbf{x}^\top \mathbf{y}$.

The following theorem establishes the key properties of the estimator formed by these embeddings.

THEOREM 3.1 (UNBIASED INNER PRODUCT ESTIMATOR). *Let $\mathbf{b}_i$ and $\mathbf{b}_j$ be the randomized Fourier embeddings of $\tilde{\mathbf{a}}_i$ and $\tilde{\mathbf{a}}_j$, respectively, as defined by Equation 3. Then, the complex inner product $\langle \mathbf{b}_i, \mathbf{b}_j \rangle = \mathbf{b}_i^* \mathbf{b}_j$ is an unbiased estimator of the true inner product:*

$$\mathbb{E}_\Phi[\mathbf{b}_i^* \mathbf{b}_j] = \tilde{\mathbf{a}}_i^\top \tilde{\mathbf{a}}_j. \quad (5)$$

Furthermore, the variance of the estimator decays linearly with the embedding dimension k:

$$\text{Var}(\mathbf{b}_i^* \mathbf{b}_j) = O(1/k). \quad (6)$$

This theorem provides the foundational pillars for our method's efficiency: unbiasedness, concentration, and complexity reduction. The **unbiasedness** of the approximated inner product ensures that its expectation is exact, which guarantees that downstream analysis—such as the eigen-decomposition of the approximated covariance matrix $\mathbf{B}^* \mathbf{B}$—converges to the correct result in expectation, thereby delivering the *energy preservation guarantee*. Furthermore, the **concentration** property ensures that the variance of the estimator decreases linearly with the embedding dimension k; through Johnson-Lindenstrauss-type arguments [26] and concentration inequalities, the approximation error for all pairwise inner products is tightly bounded with high probability even for a modest embedding dimension scaling as $k \sim O(\log M)$. Finally, the drastic **complexity reduction** transforms the computational burden: instead of constructing an $N \times N$ matrix at a prohibitive cost of $O(N^2 M)$, we now build a $N \times k$ matrix $\mathbf{B}$ (where $k \ll M, N$).

This randomized embedding transforms an intractable quadratic problem into a manageable linear one, enabling the analysis of massively large datasets while providing strong theoretical guarantees on the preservation of the data's geometric structure.

A consequence of this random projection is that the Johnson-Lindenstrauss lemma holds. For a target dimension $k = O(\epsilon^{-2} \log M)$, all pairwise inner products are preserved within an ϵ-factor with high probability:

$$\mathbb{P}\left(\left|\langle \mathbf{b}_i, \mathbf{b}_j \rangle - \langle \tilde{\mathbf{a}}_i, \tilde{\mathbf{a}}_j \rangle\right| \geq \epsilon \|\tilde{\mathbf{a}}_i\| \|\tilde{\mathbf{a}}_j\|\right) \leq 2e^{-k\epsilon^2/4} \tag{7}$$

Efficient Computation using the FFT:. The operation $\tilde{\mathbf{a}}_i \mathbf{\Phi}^\top$ is equivalent to taking a random Fourier transform of the signal $\tilde{\mathbf{a}}_i$. For each term vector $\tilde{\mathbf{a}}_i$ (a sparse vector of length M), the computational cost is $O(k \log M)$ using the Non-Uniform FFT (NUFFT) [20] or similar algorithms, where the $\log M$ factor arises from interpolating the sparse signal onto a regular grid for an FFT. The total cost for all N terms is therefore $O(Nk \log M)$.

Storage: The embedding matrix $\mathbf{B} \in \mathbb{C}^{k \times N}$ requires $O(kN)$ storage. This is a massive reduction from $O(NM)$ because $k \ll M$ (e.g., $k \sim 1000$–10000, while N can be in the billions).

3.3 Cross-Power Spectral Density Estimation with Phase Analysis

Having projected the high-dimensional, centered term vectors $\tilde{\mathbf{a}}_i$ into the low-dimensional complex space via the randomized Fourier embedding $\mathbf{b}_i = \frac{1}{\sqrt{k}} \mathbf{\Phi} \tilde{\mathbf{a}}_i$, we now construct a similarity matrix in this embedded space. We define the *Cross-Power Spectral Density (CPSD)* matrix $\mathbf{P} \in \mathbb{C}^{N \times N}$ for the embedded terms [3]. The entries of $\mathbf{P}$ are given by the complex inner products of the embeddings:

$$P_{ij} = \langle \mathbf{b}_i, \mathbf{b}_j \rangle = \mathbf{b}_i^* \mathbf{b}_j \tag{8}$$

This matrix is Hermitian ($\mathbf{P} = \mathbf{P}^*$) and serves as a statistically well-founded proxy for the matrix $\mathbf{G} = \tilde{\mathbf{A}} \tilde{\mathbf{A}}^\top$.

Theoretical Justification: From CPSD to Correlation. The following theorem formalizes the connection between the CPSD matrix and the desired correlation coefficients, providing the core justification for our approach.

THEOREM 3.2 (CPSD CORRELATION ESTIMATOR). *Let $\mathbf{b}_i$ and $\mathbf{b}_j$ be the randomized Fourier embeddings of the centered term vectors $\tilde{\mathbf{a}}_i$ and $\tilde{\mathbf{a}}_j$, respectively. Let $P_{ij} = \mathbf{b}_i^* \mathbf{b}_j$ be their Cross-Power Spectral Density. Then, the estimator:*

$$\hat{\rho}_{ij} = \frac{\Re(P_{ij})}{\sqrt{P_{ii}} \sqrt{P_{jj}}} \tag{9}$$

is a consistent estimator for the true Pearson correlation coefficient ρ_{ij} between terms i and j. That is, $\hat{\rho}_{ij} \xrightarrow{p} \rho_{ij}$ as the embedding dimension $k \to \infty$. $\Re(P_{ij})$ takes the real part of the complex-valued inner product.

The Informative Role of Phase. A significant advantage of operating in the complex plane is the rich information encoded in the *phase* of the CPSD entries. For a complex value $P_{ij} = |P_{ij}| e^{i\theta_{ij}}$, the phase $\theta_{ij} = \arg(P_{ij})$ provides immediate directional insight into the relationship between terms i and j:

---
[3]This matrix will not be computed nor materialized in the sequel.

- $\theta_{ij} \approx 0$: The complex vectors $\mathbf{b}_i$ and $\mathbf{b}_j$ are nearly in phase. This indicates a *positive correlation* between the original terms; their embeddings point in roughly the same direction in $\mathbb{C}^k$.
- $\theta_{ij} \approx \pi$ (180°): The vectors are in anti-phase. This indicates a *negative correlation* (anti-correlation); when one term is prominent, the other is likely absent.
- $\theta_{ij} \approx \pm\pi/2$ (±90°): The vectors are orthogonal in the complex plane. Their real inner product $\Re(P_{ij})$ is near zero, indicating *linear independence* or orthogonality, suggesting the terms are uncorrelated.

This phase analysis offers an intuitive, geometric interpretation of the estimated correlations directly from the complex-valued $\mathbf{P}$ matrix, often allowing for qualitative analysis without explicitly computing the normalized ratio $\hat{\rho}_{ij}$ for every pair.

Non-Asymptotic Error Bounds. The quality of the estimation is not merely asymptotic; it comes with strong, non-asymptotic probabilistic guarantees crucial for applications.

LEMMA 3.3 (ERROR BOUND FOR CORRELATION ESTIMATION). *For any pair (i, j), any embedding dimension k, and any confidence parameter $\delta \in (0, 1)$, the error of the correlation estimator is bounded with high probability:*

$$\mathbb{P}\left(|\hat{\rho}_{ij} - \rho_{ij}| \leq C\sqrt{\frac{\log(1/\delta)}{k}}\right) \geq 1 - \delta \tag{10}$$

where C is a constant independent of N and M.

This bound, which is derivable from concentration inequalities is critical for two reasons. First, it confirms that the estimation error decreases at a rate of $O(1/\sqrt{k})$ as the embedding dimension k increases. Second, and more importantly, it provides a rigorous mechanism for selecting the embedding dimension k based on a desired error tolerance ϵ and confidence level δ. Solving the inequality $C\sqrt{\frac{\log(1/\delta)}{k}} \leq \epsilon$ for the parameter k yields the requirement $k \geq \frac{C^2 \log(1/\delta)}{\epsilon^2}$. The logarithmic dependence on the confidence parameter δ and the inverse quadratic dependence on the error tolerance ϵ are precisely what make this randomized approach both scalable and practical for large-scale applications.

Algorithmic Implication and Complexity. While the Cross-Power Spectral Density (CPSD) matrix $\mathbf{P} = \mathbf{B}\mathbf{B}^*$ provides the theoretical foundation for correlation estimation, its explicit construction presents a significant computational bottleneck. The computation of this $N \times N$ Hermitian matrix requires calculating the inner products between all pairs of the N term embeddings, leading to a time complexity of $O(N^2 k)$. This quadratic scaling in the vocabulary size N renders the direct approach infeasible for large-scale applications where N can be in the millions. In the following section, we will demonstrate how to circumvent this prohibitive cost by leveraging sparse recovery techniques, which allow us to accurately estimate the correlation for each term without ever explicitly constructing the full $\mathbf{P}$ matrix.

4 Sparse Correlation Recovery via Compressed Sensing

A central challenge in our setting is efficiently discovering correlations between a term and all other terms in the dataset. The naive approach of computing all pairwise correlations is computationally prohibitive for large N, scaling as $O(N^2)$. However, a key insight underpinning our method is the *sparsity-of-effects* principle: in most instances, a given term w_i interacts significantly with only a small number, $S \ll N$, of other terms. The correlation vector $\boldsymbol{\rho}_i = (\rho_{i1}, \ldots, \rho_{iN})^\top$ is therefore S-**sparse** or approximately sparse.

We leverage this sparsity by reformulating the correlation recovery problem as a **Compressed Sensing (CS)** task [8, 43]. Instead of measuring all N potential correlations directly, we acquire a small number of **compressed measurements** $k \ll N$ and use convex optimization to infer the sparse correlation vector.

4.1 Sparse Recovery via Orthogonal Matching Pursuit

For each term w_i, we recover its correlation vector by formulating the recovery as an Orthogonal Matching Pursuit (OMP) problem [18]. This formulation is amenable to an iterative solution that provides a computationally efficient alternative to convex optimization. Instead of solving a single minimization problem, OMP greedily constructs the sparse solution vector $\mathbf{x}_i \in \mathbb{R}^N$ over S steps, where S is the target sparsity.

The algorithm maintains a residual vector $\mathbf{r}$, initialized as the measurement vector $\mathbf{z}_i$. In each step, it performs two key operations:

(1) **Identification:** It searches for the column $\boldsymbol{\psi}_j$ in the sensing matrix $\boldsymbol{\Psi}$ that is most correlated with the current residual $\mathbf{r}$.
(2) **Projection:** It adds this column to an active set and then calculates the least-squares solution for the coefficients of all currently active columns, ensuring an optimal fit at each step. The residual is then updated by subtracting this new fit.

Let us dissect the components of this process. The solution vector $\hat{\mathbf{x}}_i$ that serves as an estimate for the true correlation vector $\boldsymbol{\rho}_i$ is built iteratively. The **identification step** greedily finds the most significant correlation at each stage. The **projection step** is crucial as it ensures the solution remains consistent with the observed measurements $\mathbf{z}_i$ by minimizing the error $\|\boldsymbol{\Psi}\mathbf{x}_i - \mathbf{z}_i\|_2$ over the set of chosen correlations. This greedy construction avoids the high computational cost of ℓ_1-minimization while still effectively leveraging the signal's underlying sparsity.

4.2 Sensing Matrix and Measurement Vector

The efficacy of the compressed sensing approach critically depends on the design of the **sensing matrix** $\boldsymbol{\Psi}$ and the **measurement vector** $\mathbf{z}_i$.

The sensing matrix $\boldsymbol{\Psi} \in \mathbb{C}^{k \times N}$ is constructed from normalized measurement vectors (computed in Section 3.2) and is formally defined as:

$$\boldsymbol{\Psi} = \left[\frac{\mathbf{b}_1}{\sqrt{P_{11}}}, \frac{\mathbf{b}_2}{\sqrt{P_{22}}}, \ldots, \frac{\mathbf{b}_N}{\sqrt{P_{NN}}} \right]^\top . \tag{11}$$

Each column j of $\boldsymbol{\Psi}$ corresponds to a term w_j and is given by $\mathbf{b}_j/\sqrt{P_{jj}}$. The normalization by $\sqrt{P_{jj}}$, which approximates the standard deviation of term w_j's vector,[4] is crucial as it ensures that the energy of each column is controlled—a necessary condition for the theoretical recovery guarantees. This matrix acts as a linear projection operator that maps the high-dimensional correlation vector $\boldsymbol{\rho}_i \in \mathbb{R}^N$ down to the low-dimensional measurement space $\mathbb{C}^k$.

The corresponding measurement vector for term w_i is defined as $\mathbf{z}_i = \mathbf{b}_i/\sqrt{P_{ii}} \in \mathbb{C}^k$. This vector represents the observed compressed measurement. The entire system is designed such that this observation approximates a linear combination of the correlations ρ_{ij} between w_i and all other terms w_j, sensed through the matrix $\boldsymbol{\Psi}$:

$$\mathbf{z}_i \approx \boldsymbol{\Psi}\boldsymbol{\rho}_i = \sum_{j=1}^{N} \rho_{ij} \cdot \frac{\mathbf{b}_j}{\sqrt{P_{jj}}}. \tag{12}$$

This approximation contains noise and errors inherent in the embedding process, which we can model as an error vector $\mathbf{e}$ such that $\mathbf{z}_i = \boldsymbol{\Psi}\boldsymbol{\rho}_i + \mathbf{e}$. A standard result in compressed sensing theory is that the expected energy of this stochastic error, $\|\mathbf{e}\|_2$, scales with the number of measurements as $O(\sqrt{k})$ [18]. The OMP algorithm is robust to this error, which is explicitly accounted for in its theoretical guarantees.

4.3 Theoretical Guarantee: Stable Sparse Recovery

The power of this greedy approach is justified by the following theorem, which provides a rigorous bound on the recovery error for OMP.

THEOREM 4.1 (OMP RECOVERY GUARANTEE). *If the sensing matrix $\boldsymbol{\Psi}$ satisfies the **Restricted Isometry Property (RIP)** of order $S + 1$ with a sufficiently small constant δ_{S+1}, then the solution $\hat{\mathbf{x}}_i$ produced by the OMP algorithm after S steps satisfies:*

$$\|\hat{\mathbf{x}}_i - \boldsymbol{\rho}_i\|_2 \leq C_1 \|\mathbf{e}\|_2 + C_2 \frac{\|\boldsymbol{\rho}_i - \boldsymbol{\rho}_i^S\|_1}{\sqrt{S}} \tag{13}$$

where $\mathbf{e}$ is the noise vector from the measurement model, $\boldsymbol{\rho}_i^S$ is the best S-term approximation of $\boldsymbol{\rho}_i$, and C_1, C_2 are constants.

Interpretation of the Guarantee: The provided recovery guarantee has two key interpretations. First, the role of the **Restricted Isometry Property (RIP)** is fundamental. This condition requires that the sensing matrix $\boldsymbol{\Psi}$ acts as a near-isometry, meaning it approximately preserves the lengths of all sparse vectors. This geometric preservation is crucial as it ensures the greedy selections made by OMP are reliable, preventing distinct sparse vectors from being mapped to the same compressed measurement. Random matrices, including the constructed Fourier-based matrix $\boldsymbol{\Psi}$, are known to satisfy the RIP with high probability when the number of measurements scales as $k = O(S \log(N/S))$ [5, 8].

Second, the error bound itself decomposes into two interpretable components. The term $C_1\|\mathbf{e}\|_2$ constitutes the noise term. As established previously, the energy of the error vector $\|\mathbf{e}\|_2$ is expected to scale as $O(\sqrt{k})$, so this term quantifies how the recovery error scales

---

[4] b_j is zero mean and $\sigma_j^2 = \frac{1}{k}\sum_{i=1}^{k}|b_{ji}|^2 = P_{jj}$

with noise in the measurement process. The term $C_2 \|\rho_i - \rho_i^S\|_1/\sqrt{S}$ is the approximation term. This term is zero if the true correlation vector ρ_i is exactly S-sparse. If ρ_i is instead *compressible* (meaning its coefficients decay rapidly, allowing for a good S-term approximation), this term remains small. This demonstrates the stability and robustness of the OMP algorithm, as the error degrades gracefully for vectors that are not perfectly sparse.

4.4 Practical Implementation

The core computational challenge is executing the OMP algorithm for each term. Naively running OMP against all N other terms is prohibitive, carrying a cost of at least $O(N^2 Sk)$. To achieve feasibility, we first precompute an approximate L-Nearest Neighbor (L-NN) graph in the embedding space [19, 29, 48, 51], which allows us to restrict the recovery problem for each term to a small candidate set of $L \ll N$ neighbors.

At this stage, one might consider a simpler heuristic: computing direct correlations (e.g., dot products) with these L neighbours, which we will refer to as the Craft with dot product baseline (Craft-DP). While computationally efficient , this approach has critical drawbacks that our sparse recovery formulation overcomes. The primary advantages of using OMP on the candidate set are:

- **Denoising and Robustness:** The simple heuristic is sensitive to noise, as geometric proximity in the embedding space may not reflect true correlation. OMP's model-based approach ($z_i \approx \Psi \rho_i$) acts as a powerful denoising filter, identifying the candidates that form the most consistent and signal-rich explanation.
- **Discovery of Non-Redundant Factors:** The simple heuristic evaluates each neighbor independently, often producing a list of highly correlated, redundant terms (e.g., "database", "SQL", "RDBMS"). OMP, by contrast, considers all candidates simultaneously. It naturally produces a parsimonious result by "explaining away" the influence of other terms once a primary correlate has been chosen, thereby revealing a more fundamental set of drivers.

For the OMP algorithm on the restricted set of L neighbors, the total cost plummets to a tractable $O(NSLk)$. This is linear in the number of terms N. The final output is a sparse graph requiring $O(NL)$ storage. To empirically validate our claims, we present an experimental comparison of our proposed method against Craft-DP in section 6.

4.5 Statistical Significance Testing and Multiple Testing Correction

In large-scale correlation analyses, the sheer number of pairwise tests performed—on the order of $O(N^2)$—inevitably leads to a high number of false positives if statistical significance is not rigorously assessed. Without proper correction, many spurious correlations may be mistakenly identified as meaningful, undermining the reliability of the results. Therefore, we incorporate a two-stage statistical testing procedure: first, we assess the significance of each individual correlation estimate, and second, we apply a multiple testing correction to control the overall false discovery rate across the entire set of hypotheses.

For each estimated correlation $\hat{\rho}_{ij}$, we test the null hypothesis $H_0 : \rho_{ij} = 0$. We apply Fisher's z-transform to transform the raw estimates into a statistic and stabilize the variance of the correlation coefficient:

$$z_{ij} = \frac{1}{2} \log \left(\frac{1 + \hat{\rho}_{ij}}{1 - \hat{\rho}_{ij}} \right) \tag{14}$$

Under H_0, the statistic z_{ij} is approximately normally distributed with mean 0 and variance $\frac{1}{k-3}$ (where k is the embedding dimension). The resulting test statistic $T_{ij} = z_{ij}\sqrt{k-3}$ therefore follows a standard normal distribution, $T_{ij} \sim \mathcal{N}(0, 1)$. This allows us to compute two-tailed p-values in the standard way.

Given the $O(N^2)$ hypotheses being tested, a multiple testing correction is imperative to control the false positive rate. We control the False Discovery Rate (FDR) using the Benjamini-Hochberg procedure [6]. For a fixed term w_i, let $p_{(1)} \leq p_{(2)} \leq \cdots \leq p_{(m)}$ be the sorted p-values of all its m tested correlations. We find the largest index r such that:

$$p_{(r)} \leq \frac{r}{m} \alpha \tag{15}$$

We then reject all hypotheses corresponding to $p_{(1)}, \ldots, p_{(r)}$, where α is the desired significance level (e.g., 0.05). The threshold $p_{\text{BH}} = p_{(r)}$ serves as the corrected significance level for term w_i.

The final output of our algorithm is a set of significant term pairs that meet both a strength and a significance criterion:

$$E = \left\{ (w_i, w_j) : |\hat{\rho}_{ij}| > \tau \quad \text{and} \quad p_{ij} \leq p_{\text{BH}} \right\} \tag{16}$$

where τ is a correlation strength threshold.

Complexity Analysis. The complexity of the algorithm is dominated by the initial signal embedding stage. The randomized Fourier transform takes $O(Nk \log M)$. The subsequent stages are computationally less expensive. The sparse correlation recovery via OMP is performed for each of the N terms on a restricted candidate set of size L. With a target sparsity of S, this recovery has a total time complexity of $O(NSLk)$.

The final statistical validation phase consists of two steps. First, calculating a p-value using the Fisher z-transform for each of the (at most) S non-zero correlations per term takes $O(NS)$ time in total. Second, applying the Benjamini-Hochberg procedure requires sorting these S p-values for each of the N terms, resulting in a total cost of $O(NS \log S)$.

5 THE CRAFT SYSTEM FRAMEWORK

We now present our proposed framework, **CRAFT (Corpus Relatedness Analysis Using Fourier Transforms)**. Our core insight is to re-cast the problem of large-scale term relatedness discovery from a high-dimensional statistical challenge to a low-dimensional signal processing task. We treat the presence of a given term across the corpus's M documents as a discrete signal. Semantically related terms will exhibit correlated patterns within their respective signals. We hypothesize that these correlations can be robustly identified in the compact frequency domain, bypassing the quadratic cost of direct comparison in the original term-document space.

5.1 The CRAFT Architecture

To operationalize our insight, we designed CRAFT as a scalable, three-stage data pipeline. As illustrated in Figure 2, this architecture
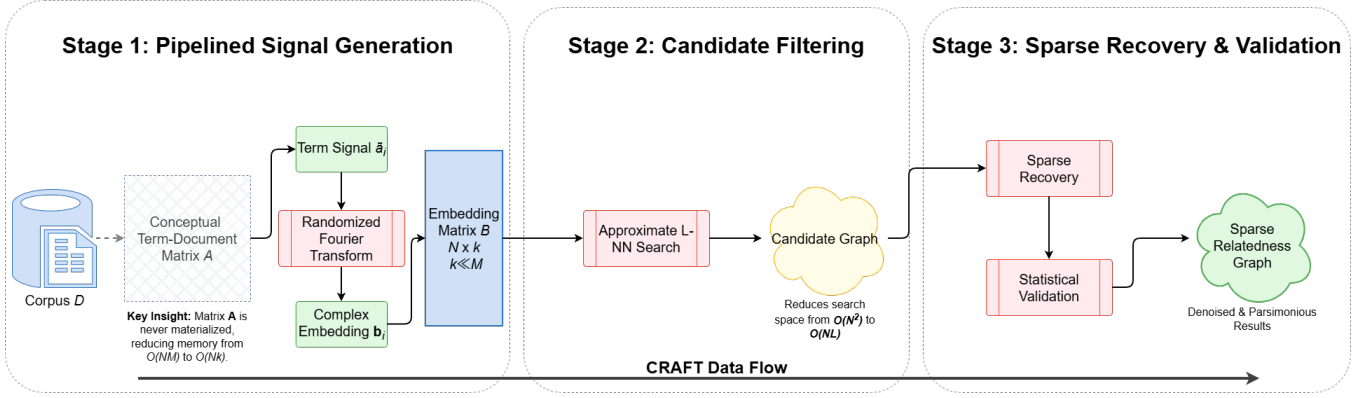
Figure 2: The CRAFT system architecture, illustrating the three main stages: 1) Pipelined Signal Generation and Embedding, 2) Candidate Filtering via Approximate k-NN, and 3) Sparse Recovery and Statistical Validation.

transforms the sparse text corpus into a low-dimensional representation where we can efficiently identify a small set of candidate correlations, which are then robustly recovered and validated. The implementation of this end-to-end process is formally detailed in Algorithm 1.

Stage 1: Pipelined Signal Generation and Embedding. The first stage of CRAFT, corresponding to lines 3-9 of Algorithm 1, transforms the raw text corpus $\mathcal{D}$ directly into a dense, low-dimensional complex embedding matrix $\mathbf{B}$, where each row represents a term. This is achieved through a pipelined process that is conceptually two-part:

(1) **Signal Definition:** For each term w_i in the vocabulary $\mathcal{V}$, we first define its corresponding M-dimensional signal. This process begins with standard vocabulary construction (tokenization, pruning, etc.) and uses the BM25 weighting function (Equation (1)) to define a conceptual term-document matrix $\mathbf{A}$. The final signal for term w_i, denoted $\tilde{\mathbf{a}}_i$, is the corresponding mean-centered row of this conceptual matrix.

(2) **Randomized Fourier Embedding:** As each high-dimensional signal $\tilde{\mathbf{a}}_i$ is generated, it is immediately projected into a k-dimensional complex embedding $\mathbf{b}_i$ via the Randomized Fourier Transform (Equation (3)). This projection provably preserves the inner product information essential for our analysis (Theorem 3.1).

This integrated pipeline is the key to our framework's scalability. By generating and immediately embedding each signal in the loop spanning lines 5-9, the conceptual $N \times M$ term-document matrix $\mathbf{A}$ is **never explicitly materialized**. This approach provides a significant performance benefit, **reducing the memory footprint from a prohibitive $O(NM)$ to a tractable $O(Nk)$**, as $k \ll M$. The final $N \times k$ matrix $\mathbf{B}$ is constructed directly, enabling CRAFT to process massive corpora on commodity hardware.

Stage 2: Candidate Filtering via Approximate k-NN. A naive $O(N^2 k)$ all-pairs comparison on the embedding matrix $\mathbf{B}$ is intractable. Based on the **sparsity-of-effects hypothesis**—that any term is only meaningfully related to a few others—we reframe this as an efficient candidate filtering problem. This stage is detailed in **lines**

10-16 of Algorithm 1. The goal is to find, for each term w_i, a small candidate set $\mathcal{L}_i$ of its $L \ll N$ most likely interaction partners.

This task is equivalent to a large-scale **Approximate k-Nearest Neighbor (ANN)** search. Our implementation first normalizes the embedding vectors (**line 10**) and then uses **Faiss** [15], a high-performance similarity search library, to build a **Hierarchical Navigable Small Worlds (HNSW)** [31] index on the normalized vectors (**line 11**). We chose HNSW for its exceptional query speed, which is ideal for our "build-once, query-N-times" workload. By querying this index for each of the N terms in the loop at **lines 13-16**, we find the L nearest neighbors for each term (**line 14**) and generate a candidate graph that reduces the search space from $O(N^2)$ to a tractable $O(NL)$.

Stage 3: Sparse Recovery via Orthogonal Matching Pursuit. The final stage, which covers **lines 17-38**, takes the candidate graph and recovers a sparse set of high-quality correlations for each term. Instead of convex optimization, we adopt the Orthogonal Matching Pursuit (OMP) solver, a computationally efficient greedy algorithm that is robust to the noise inherent in the embedding process.

For each term w_i, as processed in the main loop (**lines 19-38**), we solve for its sparse correlation vector $\mathbf{x}_i$ from the model $\mathbf{z}_i \approx \mathbf{\Psi}_{\mathcal{L}_i} \mathbf{x}_i$. Here, $\mathbf{z}_i$ is the normalized embedding for w_i (**line 21**) and the sensing matrix $\mathbf{\Psi}_{\mathcal{L}_i}$ is constructed from the embeddings of its L candidates (**line 22**), using the full transposed matrix $\mathbf{\Psi}$ created on **line 18**. The SolveOMP function is called to recover the sparse vector of correlations $\hat{\mathbf{x}}_i^{\mathcal{L}}$ (**line 23**). OMP runs for a fixed number of iterations, S (the target sparsity). In each iteration, it performs two steps: 1) **Identification**, where it selects the candidate term that is most correlated with the current residual, and 2) **Projection**, where it computes a new least-squares solution over all currently selected candidates to update the coefficients and residual.

Following recovery, the identified non-zero correlations $\hat{\rho}_{ij}$ undergo rigorous statistical validation. For each potential correlation, a p-value p_{ij} is computed via Fisher's z-transform (**line 27**). To account for the large number of tests, we apply the Benjamini-Hochberg procedure to control the false discovery rate at a given significance level α (**line 32**). Only those correlations whose p-values are below the corrected threshold are deemed statistically

---

Algorithm 1 The End-to-End CRAFT Pipeline

1: **Input:** Corpus $\mathcal{D}$, Embedding dim. k, Neighbor set size L, Significance level α
2: **Output:** Set of significant correlated pairs E
3: $\mathcal{V} \leftarrow$ BuildVocabulary($\mathcal{D}$)
4: $\mathbf{B} \leftarrow$ zeros(N, k, dtype=complex)
5: **for** each term $w_i \in \mathcal{V}$ (from $i = 1$ to N) **do**
6: $\quad \tilde{\mathbf{a}}_i \leftarrow$ GenerateCenteredSignal($\mathcal{D}, w_i$)
7: $\quad \mathbf{b}_i \leftarrow$ ApplyRFT($\tilde{\mathbf{a}}_i$)
8: $\quad \mathbf{B}[i,:] \leftarrow \mathbf{b}_i^\top$
9: **end for**
10: $\mathbf{B}_{\text{norm}} \leftarrow$ NormalizeRows($\mathbf{B}$)
11: FaissIndex $\leftarrow$ BuildHNSWIndex($\mathbf{B}_{\text{norm}}$)
12: $\mathcal{L} \leftarrow$ new map()
13: **for** each term $w_i \in \mathcal{V}$ (from $i = 1$ to N) **do**
14: $\quad \mathcal{L}_i \leftarrow$ FaissIndex.Search($\mathbf{B}_{\text{norm}}[i,:], L$)
15: $\quad \mathcal{L}[i] \leftarrow \mathcal{L}_i$
16: **end for**
17: $E \leftarrow \emptyset$
18: $\boldsymbol{\Psi} \leftarrow \mathbf{B}_{\text{norm}}^\top$
19: **for** each term $w_i \in \mathcal{V}$ (from $i = 1$ to N) **do**
20: $\quad \mathcal{L}_i \leftarrow \mathcal{L}[i]$
21: $\quad \mathbf{z}_i \leftarrow \boldsymbol{\Psi}[:, i]$
22: $\quad \boldsymbol{\Psi}_{\mathcal{L}_i} \leftarrow \boldsymbol{\Psi}[:, \mathcal{L}_i]$
23: $\quad \hat{\mathbf{x}}_i^{\mathcal{L}} \leftarrow$ SolveOMP($\boldsymbol{\Psi}_{\mathcal{L}_i}, \mathbf{z}_i, S$)
24: $\quad$ p_values $\leftarrow$ []
25: $\quad$ results $\leftarrow$ []
26: $\quad$ **for** each non-zero $\hat{\rho}_{ij}$ in $\hat{\mathbf{x}}_i^{\mathcal{L}}$ (with index $j \in \mathcal{L}_i$) **do**
27: $\qquad p_{ij} \leftarrow$ FisherZTest($\hat{\rho}_{ij}, M$)
28: $\qquad$ p_values.append(p_{ij})
29: $\qquad$ results.append($(i, j, \hat{\rho}_{ij}, p_{ij})$)
30: $\quad$ **end for**
31: $\quad p_{\text{BH}} \leftarrow$ BenjaminiHochberg(p_values, α)
32: $\quad$ **for** $(i, j, \hat{\rho}_{ij}, p_{ij}) \in$ results **do**
33: $\qquad$ **if** $p_{ij} \leq p_{\text{BH}}$ **then**
34: $\qquad\quad E \leftarrow E \cup \{(w_i, w_j)\}$
35: $\qquad$ **end if**
36: $\quad$ **end for**
37: **end for**
38: **return** E

---

significant and are added to the final output set E (**lines 33-37**). This set of significant correlated pairs is the final output of the pipeline. This model-based recovery acts as a powerful denoising filter and produces a parsimonious set of non-redundant factors. Since this entire process is run independently for each term on its restricted candidate set, it is embarrassingly parallel and computationally tractable.

6 Experimental Evaluation

In this section, we present a comprehensive empirical evaluation of CRAFT. Our experiments are designed to answer the following key research questions:

- **Effectiveness:** How does the quality of the term correlations discovered by CRAFT compare to alternative and baseline methods?
- **Efficiency & Scalability:** How do the runtime and memory requirements of CRAFT scale with the size of the corpus and vocabulary?
- **Ablation Study:** How do the core components of CRAFT contribute to its overall performance, and how sensitive is the model to its key hyperparameters?

6.1 Experimental Setup

Our experimental design is structured to rigorously evaluate CRAFT's performance across two primary dimensions: **effectiveness** and **efficiency**. For effectiveness, we evaluate all methods under two distinct scenarios: (1) a **ranked retrieval** task where the generated candidate pairs are ordered by the similarity score, and (2) a **significance set** task where a statistical test is used to select a final set of pairs. To support this comprehensive evaluation, we employ two categories of datasets.

6.1.1 Benchmark Datasets for Effectiveness Evaluation. To evaluate effectiveness, we employ two standard knowledge graph construction benchmarks from the Text2KG suite [41], both of which provide ground-truth triples for each text document. Their well-structured nature and moderate scale are ideal for a precise quantitative and qualitative analysis of the discovered correlations.

- **Wikidata-TekGen:** A dataset of 13K documents synthesized from Wikidata triples. It is characterized by a broad, general-domain vocabulary of entities and relations.
- **DBpedia-WebNLG:** A corpus of 4K documents containing descriptive, well-structured sentences generated from DBpedia triples, providing a clean and varied evaluation setting.

6.1.2 Large-Scale Corpora for Scalability Evaluation. To address efficiency and scalability, we also test our approach on two large corpora that are representative of challenging, large-scale text. Their significant size allows us to thoroughly test the performance of CRAFT.

- **GenWiki:** A large-scale, general-domain dataset constructed from English Wikipedia[25]. Comprising over 700K articles. It was created for KG construction with golden triplet and to overcome the limitations of smaller supervised datasets for unsupervised models.
- **arXiv Corpus:** To evaluate performance on domain-specific scientific text at scale, we use a series of corpora constructed from text chunks extracted from full-text computer science papers from arXiv[12]. Characterized by a specialized vocabulary, these serve as a robust benchmark. We use three versions of increasing size: **arXiv-1M** (1 million text chunks), **arXiv-3M** (3 million chunks), and **arXiv-5M** (5 million chunks).

6.1.3 Compared Methods. To rigorously evaluate our framework, we compare the full CRAFT pipeline against a series of methods. To ensure a fair comparison of the embedding and recovery stages, all methods leverage the same Approximate Nearest Neighbor (ANN)

Table 1: Effectiveness on all datasets, measured by Mean Average Precision (mAP) and F1-Score.

Method	Wikidata		DBpedia		GenWiki		arXiv-1M		arXiv-3M		arXiv-5M	
	mAP	F1	mAP	F1	mAP	F1	mAP	F1	mAP	F1	mAP	F1
RP-ANN	92.7	46.1	97.2	51.2	80.5	42.5	75.3	40.1	74.1	39.5	73.5	39.0
SVD-ANN	95.1	33.6	99.1	40.1	81.2	40.8	77.8	38.4	76.5	37.9	75.9	37.1
CRAFT-DP	99.3	80.1	99.2	78.5	83.6	80.6	82.1	78.2	80.9	77.8	80.5	77.1
CRAFT	98.7	80.5	98.1	80.3	85.0	81.3	80.9	80.5	81.1	79.9	80.1	79.2

search component [19, 29, 48] for candidate filtering. The following methods are evaluated:

(1) **RP-ANN:** This method represents a standard, scalable heuristic. It first builds a term-document matrix with BM25 weights, applies a **Random Projection (RP)** [3] to reduce dimensionality, and then performs the ANN search.

(2) **SVD-ANN:** This baseline applies a truncated **Singular Value Decomposition (SVD)** to the BM25 matrix (similar to the classic Latent Semantic Analysis method []), to generate dense embeddings for the subsequent ANN search.

(3) **CRAFT-DP:** This variant first applies the CRAFT Fourier embedding and ANN filtering stages. It then isolates our final stage by replacing the OMP sparse recovery step with a simple dot product ranking on the candidate set, allowing us to quantify the benefit of OMP as part of our ablation study.

(4) **CRAFT:** This is our full, end-to-end proposed framework, including the initial Fourier embedding, the ANN candidate filtering, and the final sparse correlation recovery via Orthogonal Matching Pursuit.

6.1.4 Evaluation Metrics & Implementation.

- **Effectiveness:** We evaluate the quality of the discovered term pairs under the two scenarios based on the output format:
  - **Ranked List Evaluation:** For the ranked retrieval task, we report **Mean Average Precision (mAP)**. This metric is the mean of the Average Precision (AP) scores over a set of queries Q, defined as:

$$\text{mAP} = \frac{1}{|Q|} \sum_{q \in Q} \text{AP}(q)$$

  where $\text{AP}(q)$ for a single query is the average of precision values at the position of each correct item in the ranked list. A higher mAP score indicates better performance, as it rewards models for placing correct items at the top of the list.
  - **Significance Set Evaluation:** For the significance set task, we report **F1-Score**.

A rigorous evaluation of correlation-based discovery methods requires a ground truth that is methodologically aligned with the chosen statistical metric. Accordingly, we construct our benchmark to consist exclusively of pairs that exhibit a strong statistical association as measured by the Pearson correlation coefficient.

To this end, we operationally define a strong correlation as any pair with a Pearson score at or above the 95th percentile among all the possible pairs. This threshold is applied universally to ensure consistency:

- For datasets providing a golden set, we perform a refinement, retaining only those golden pairs that meet our 95th percentile criterion.
- For datasets without a golden set, this threshold is used to construct the ground truth directly.

This principled methodology guarantees that our benchmark is composed of a high-confidence set of pairs, ensuring the evaluation is a valid and precise measure of a system's ability to detect strong correlations.

- **Efficiency:** To characterize system performance, we measure both end-to-end wall-clock time and peak memory usage. Our analysis focuses on runtime as the primary efficiency metric, as the peak memory bottleneck is consistent across all methods.[5] This bottleneck is the storage of the final dense embedding matrix of size $N \times k$, where N is the vocabulary size and k is the embedding dimension. Since this data structure is a shared requirement for all evaluated algorithms, we adopt runtime scalability as the primary axis for our efficiency evaluation.

- **Implementation:** All experiments were conducted on a server equipped with an AMD EPYC 7C13 CPU and 512 GB of RAM. Our system is implemented in Python, utilizing NumPy, SciPy, and the Faiss library for its HNSW index. For OMP, we adopted the fast algorithm from [50]. Unless otherwise noted, the default parameters for CRAFT are an embedding dimension of $k = 256$, a neighbor set size of $L = 100$ and a significance level $\alpha = 0.05$.

6.2 Effectiveness Evaluation

We evaluate effectiveness across all four datasets, with the primary results presented in Table 1. The analysis is divided into two parts, corresponding to our two evaluation scenarios: ranking quality and the quality of the final significance set.

6.2.1 Ranking Quality. As shown in Table 1, our CRAFT variants consistently outperform the baselines across all datasets. On well-structured benchmarks like **Wikidata** and **DBpedia**, all methods achieve high mAP scores due to the clean, template-based text, with our approach reaching a near-perfect mAP of 99.3 on **Wikidata**.

---

[5]For SVD-ANN, the full term-document matrix can be prohibitively large if densified. Standard implementations, however, typically operate directly on a sparse representation of this matrix to manage memory consumption.

The performance gap widens on the more challenging large-scale datasets (**GenWiki** and **arXiv**). The complex syntax and noise in these corpora cause mAP scores to drop for all methods, highlighting the difficulty of the task. It is in these conditions, however, that **CRAFT**'s robustness becomes evident. On the largest **arXiv-5M** corpus, while baseline performance degrades significantly, CRAFT achieves an mAP of 80.1, surpassing the strongest baseline's score of 75.9. This confirms our framework's ability to produce high-quality rankings on both clean and real-world text.

6.2.2 Significance Set Quality. The F1-Score evaluates the quality of the final, discrete set of pairs deemed significant. As shown in Table 1, both of our framework's variants, **CRAFT-DP** and **CRAFT**, dramatically outperform the baselines on this metric. The baselines (**RP-ANN** and **SVD-ANN**) suffer from extremely low precision. Their underlying embeddings produce dense, noisy neighborhoods in the ANN search, resulting in an over-generation of false positive candidates. This severely harms precision and leads to poor F1-scores.

Our framework addresses this in two stages. First, the strong performance of **CRAFT-DP** indicates that the **Randomized Fourier Transform (RFT)** embeddings are inherently better at separating signal from noise. They produce a much cleaner initial candidate set from the ANN search, leading to the first substantial jump in F1-score over the baselines. Second, the full **CRAFT** model introduces the sparse recovery stage via Orthogonal Matching Pursuit (OMP). This acts as a powerful sparse recovery filter, taking the already high-quality candidate set and further refining it to prune remaining false positives. This combination—RFT for a high-quality initial set and OMP for principled final filtering—is what allows our framework to achieve its state-of-the-art F1-scores.

6.3 Efficiency and Scalability

To evaluate the practicality of CRAFT for large-scale applications, we analyze its computational performance on our two largest corpora, **GenWiki** and **arXiv** series. We separately analyze runtime and memory usage to provide a comprehensive picture of the system's efficiency.

We evaluate the end-to-end runtime, normalized against the fastest baseline, **RP-ANN**. The results in Table 2 show the relative slowdown.

The performance differences are rooted in the computational complexity of the underlying algorithms. For our **SVD-ANN** baseline, we employ a highly efficient implementation based on **randomized SVD**, which is a state-of-the-art approach for approximating the top-k singular vectors of large matrices [21]. While this randomized approach is significantly more scalable than a full decomposition, its core reliance on matrix factorization still leads to a computational bottleneck as the vocabulary and document counts grow. This explains the significant slowdown observed for SVD-ANN on the larger **arXiv** corpora.

In contrast, **CRAFT** is designed for efficiency. Its primary embedding stage uses a randomized Fourier transform, an operation related to the Fast Fourier Transform (FFT) with a near-linear time complexity. The subsequent OMP recovery step, while iterative, is only performed on small candidate sets for each term, not the entire vocabulary. Consequently, CRAFT's overall runtime remains

highly competitive, scaling nearly as well as the much less effective RP-ANN heuristic. This result is critical, as it demonstrates that CRAFT's superior effectiveness is achieved with only a minor computational overhead compared to the fastest baseline.

Table 2: Relative slowdown compared to the RP-ANN baseline on the large-scale datasets. A value of 1.0x means the runtime is identical to RP-ANN.

Method	GenWiki	arXiv-1M	arXiv-3M	arXiv-5M
RP-ANN	1.00x	1.00x	1.00x	1.00x
SVD-ANN	1.20x	1.52x	1.68x	1.85x
CRAFT-DP	1.06x	1.12x	1.15x	1.18x
CRAFT	1.15x	1.21x	1.22x	1.23x

6.4 Ablation and Comparative Analysis

We conduct an ablation study to analyze the individual contributions and computational cost of CRAFT's key components, as well as to evaluate its sensitivity to its primary hyperparameters: the embedding dimension k, the nearest neighbor list size L, and the significance level α. This study uses a subsample of the **Genwiki** dataset with 100K documents. Unless otherwise noted, the default parameters are an embedding dimension of $k = 256$, a neighbour set size of $L = 100$, and a significance level $\alpha = 0.05$.
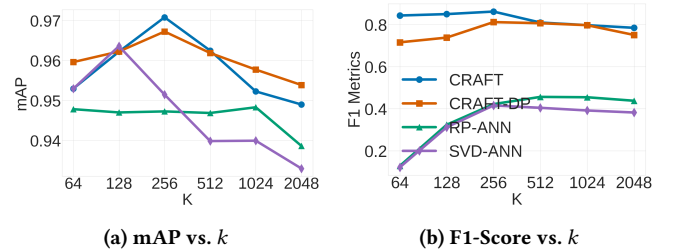

(a) mAP vs. k (b) F1-Score vs. k

Figure 3: Ablation study on the impact of embedding dimension (k) on performance.

6.4.1 Sensitivity to Embedding Dimension k. The choice of embedding dimension k presents a trade-off between expressiveness and computational cost. Our analysis shows that the effectiveness of CRAFT is robust across a wide range of k values.

As shown in Figure 3a, the ranking quality (mAP) for both **CRAFT** and **CRAFT-DP** peaks at a moderate dimension of $k = 256$. This behavior suggests that an embedding dimension of $k = 256$ effectively approximates the **intrinsic dimensionality** of the semantic space within the Genwiki dataset for this task. Dimensions smaller than this may be insufficient to capture the nuanced relationships between entities, leading to underfitting. Conversely, dimensions significantly larger than the intrinsic requirement can introduce redundancy and increase the model's capacity to overfit to noise in the training data. This likely explains the slight, gradual decrease in mAP observed for $k > 256$, as the model begins to capture spurious correlations rather than the true underlying

data structure. In contrast, the baseline methods show either lower peak performance (SVD-ANN) or relative insensitivity coupled with much lower overall effectiveness (RP-ANN).

For the significance set quality (F1-Score), shown in Figure 3b, our framework demonstrates even greater stability. After an initial sharp improvement, the F1-scores for CRAFT and CRAFT-DP remain high and plateau for all $k \geq 256$. This indicates that once the embedding dimension is sufficiently large to capture the core semantic relationships (i.e., it meets or exceeds the intrinsic dimension), the performance is not sensitive to further increases in dimensionality. This robustness is a key practical advantage, as it simplifies hyperparameter tuning.
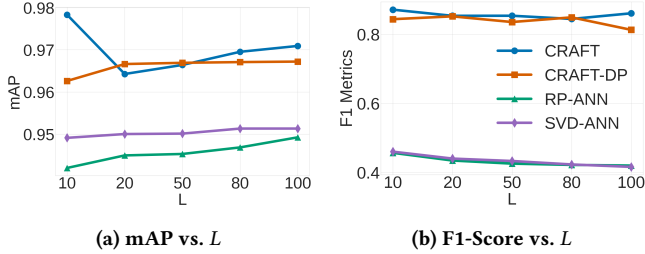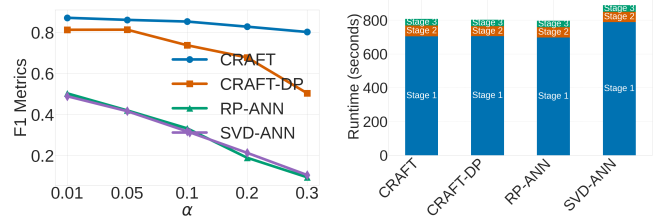

(a) mAP vs. L

(b) F1-Score vs. L

Figure 4: Ablation study on the impact of nearest neighbor list size (L) on performance.

6.4.2 Sensitivity to Nearest Neighbor List Size L. We also evaluate the model's sensitivity to the size of the nearest neighbor list, L, which is a crucial parameter for the candidate generation phase. The results show that our proposed methods maintain high performance and are remarkably stable across different values of L.

As depicted in Figure 4a, the ranking performance (mAP) of the baseline methods generally improves slightly as L increases. This is an expected outcome, as a larger candidate pool raises the potential for recall. However, **CRAFT** exhibits a more complex trend, with its high performance being less dependent on a simple expansion of the candidate list. This is because its final ranking stage does not rely on a direct dot product but instead uses Orthogonal Matching Pursuit (OMP) to find a sparse approximation of the query. OMP seeks an optimal combinatorial representation, a process not guaranteed to improve monotonically with a larger, potentially less relevant, set of candidates. The consistently superior mAP of **CRAFT** and **CRAFT-DP** across all values of L underscores the effectiveness of our overall embedding and ranking strategy.

More importantly, the quality of the significance set (F1-Score) reveals a key difference between our framework and the baselines, as shown in Figure 4b. For SVD-ANN and RP-ANN, the F1-Score tends to decrease as L grows. This suggests that these methods do not produce a **well-separated similarity measure**; there is no clear distinction between the scores of truly relevant and irrelevant entities. Consequently, increasing the candidate list size introduces more borderline candidates that are incorrectly identified as significant by the statistical test, leading to an influx of **false positives** that degrades the F1-score. In stark contrast, the F1-scores for **CRAFT** and **CRAFT-DP** remain exceptionally stable and high. This demonstrates that our framework's similarity

measure is highly discriminative, allowing it to reliably identify the core set of significant neighbours regardless of the total list size. This robustness is a valuable practical feature, enabling reliable results without extensive parameter tuning.

(a) F1-Score vs. significance level (α).

(b) Runtime breakdown per stage.

Figure 5: Ablation study on the impact of significance level (α) and a component-wise runtime analysis.

6.4.3 Sensitivity to Significance Level α. Finally, we analyze the framework's sensitivity to the significance level α, which is the threshold used in the final statistical testing phase to determine the significance set. As this test is only applied to generate the final set, this hyperparameter exclusively impacts the **F1-Score**.

Figure 5a shows the F1-Score as a function of α. For all methods, the F1-Score decreases as α becomes less strict (i.e., increases). This is because a larger α lowers the bar for statistical significance, leading to a sharp increase in the number of **false positives** being included in the final set. This influx of false positives severely degrades precision, which in turn lowers the F1-Score.

Notably, **CRAFT** demonstrates the highest F1-score and greatest robustness across all tested values, followed by **CRAFT-DP**, with both methods significantly outperforming the baselines. The superior stability of **CRAFT**, particularly as the significance threshold loosens, indicates that its OMP-based similarity measure is more discriminative than the direct dot-product approach in **CRAFT-DP**. This allows the statistical test to effectively identify true positives, which have a strong signal, without wrongly including a large number of false positives. In contrast, the performance of SVD-ANN and RP-ANN degrades rapidly, suggesting their underlying similarity scores are less reliable and not well-separated, causing the statistical test to fail.

6.4.4 Component-wise Runtime Analysis. To understand the computational costs of our framework, we analyze the runtime of each major stage for this 100k dataset, as shown in Figure 5b. The process is divided into three stages: **Stage 1** (Embedding Generation), **Stage 2** (Candidate Filtering), and **Stage 3** (Sparse Recovery/reranking with significance Testing).

The analysis reveals that Stage 1 is the dominant computational bottleneck across all methods, consuming the vast majority of the total processing time. This is expected, as generating high-dimensional embeddings are inherently expensive operations.

Among the evaluated methods, **SVD-ANN** exhibits the highest overall runtime, driven primarily by a more costly initial indexing phase in Stage 1. In contrast, **CRAFT**, **CRAFT-DP**, and **RP-ANN**

demonstrate comparable total runtimes. Notably, while CRAFT employs a more sophisticated Orthogonal Matching Pursuit algorithm in its ranking stage (Stage 3), its runtime overhead is minimal compared to the simpler dot-product re-ranking in CRAFT-DP and the baselines.

This result is significant: it shows that the substantial improvements in ranking quality (mAP) and significance set identification (F1-Score) delivered by **CRAFT** are achieved without a meaningful penalty in computational cost. The primary expense lies in the embedding and indexing stage, which is similar across most methods, while our more effective ranking and testing stages add negligible overhead.

6.4.5 Embedding Methods. To empirically distinguish semantic similarity from statistical correlation, we benchmark Model2Vec [46] against the Pearson correlation ground truth on the Wikidata dataset. By substituting the signal generation stage with pre-trained vectors while maintaining the standard retrieval protocol, we observed a distinct performance gap. Model2Vec yielded a negligible F1 score of 0.2 and mAP of 6.4, whereas CRAFT achieved 80.1 and 98.6 respectively. This performance gap highlights a fundamental objective mismatch. Embedding models optimize for predictive likelihood—grouping terms that constitute valid linguistic substitutions. While this captures broad semantic relatedness, it fails to preserve the precise, global linear co-variation required for rigorous statistical discovery. The near-random performance of embeddings on the Pearson benchmark demonstrates that semantic proximity does not imply, and often obscures, statistical correlation. Similar trends were observed across other datasets but are omitted here for brevity.

7 Related Work

The fundamental task of identifying meaningful relationships between terms in a large corpus has been a long-standing challenge in natural language processing and information retrieval.

Statistical Association Measures. A foundational approach relies on computing statistical measures from a term co-occurrence matrix, such as Pointwise Mutual Information (PMI) [11] and the Chi-Squared (χ^2) test [32]. While intuitive for individual pairs, these methods suffer from inherent quadratic scaling; evaluating all pairs across a large vocabulary requires prohibitive $O(N^2)$ computations, a classic bottleneck in data mining [16, 49]. Furthermore, PMI tends to overestimate the importance of rare term pairs, while χ^2 is difficult to interpret as a metric for association strength. In contrast, the Pearson Correlation Coefficient offers a more suitable measure for identifying consistently covarying terms. It provides a normalized, bounded score between -1 and 1 that captures both the strength and direction of linear relationships. Unlike PMI, Pearson is less sensitive to sparse counts and effectively isolates proportional co-occurrence patterns, making it a robust choice for filtering significant entity pairs.

Neural and Embedding-Based Methods. Modern approaches leverage distributional semantics, learning dense vector representations for terms from their contexts. Models like Word2Vec [34] and GloVe [39] infer relationships via cosine similarity in the embedding space. CRAFT avoids this conflation by directly estimating the Pearson correlation coefficient.

More recently, re-trained language models like BERT [14] have achieved state-of-the-art performance on supervised relation extraction tasks. However, the computational cost of training embeddings or performing inference with large models for every term pair is prohibitive for exhaustive, discovery-oriented analysis over massive corpora.

Latent Factor and Topic Models. LSA [13] applies Singular Value Decomposition (SVD) to a term-document matrix to project terms into a latent topic space. While effective, the computational complexity of performing a full SVD on a large matrix is often too expensive for truly large-scale data. Furthermore, the nature of the associations differs fundamentally: LSA relies on cosine similarity in a reduced space, which is strictly symmetric, lacks a universal scale, and reflects shared latent content. In contrast, Pearson correlation is strictly bounded between -1 and 1 and captures directional linear relationships where one variable changes predictably with the other. CRAFT bears relationship to probabilistic topic models like Latent Dirichlet Allocation (LDA), particularly regarding the exploitation of sparsity to discover latent relevance. However, the objectives remain distinct. While topic models optimize for broad semantic themes—clustering terms based on document-level co-occurrence probabilities—CRAFT is specifically designed to estimate the Pearson correlation coefficient. This focus allows CRAFT to capture precise, directional linear dependencies (distinguishing positive correlation from negative anti-correlation), rather than general thematic coherence where such directional information is often lost.

Random Projections. A highly scalable alternative is to use random projections, which are guaranteed to preserve pairwise distances between points with high probability under the Johnson-Lindenstrauss lemma [24, 26]. This involves projecting the high dimensional data onto a random lower-dimensional subspace. One could directly apply random projections to the term vectors derived from an inverted index. While feasible, this approach still requires associating N vectors, resulting in an $O(N^2)$ operation, which entails significant overheads. Our method avoids this quadratic bottleneck entirely by operating directly on the compressed frequency domain using sparse recovery techniques. Furthermore, standard random projections are designed to preserve Euclidean geometry, whereas our use of the Random Fourier Transform (RFT) is explicitly designed to create a compact sketch that preserves the frequency-domain correlations and cross-power spectral properties that are central to efficiently estimating Pearson correlation. This provides a direct and computationally advantageous link between the time-domain (token occurrences) and the desired association metric.

8 Conclusion

Discovering related terms in massive, unstructured text corpora is a critical bottleneck for applications like knowledge graph construction. We present CRAFT, a framework that overcomes this challenge by reframing term discovery as a signal processing task. CRAFT leverages randomized Fourier embeddings to compress term occurrences with theoretical guarantees, adapts Cross-Power Spectral Density (CPSD) for robust correlation estimation, and employs sparse recovery to identify significant relationships without materializing the prohibitive pairwise matrix.

References

[1] 2025. CRAFT: Corpus Relatedness Analysis Using Fourier Tranforms. https://anonymous.4open.science/r/CRAFT-FC97/.

[2] Hassan Abdallah, Béatrice Markhoff, and Arnaud Soulet. 2025. Ranking Indicator Discovery from Very Large Knowledge Graphs. *Proc. VLDB Endow.* 18, 4 (May 2025), 1183–1195. doi:10.14778/3717755.3717775

[3] Dimitris Achlioptas. 2003. Database-friendly random projections: Johnson-Lindenstrauss with binary coins. *J. Comput. System Sci.* 66, 4 (2003), 671–687. doi:10.1016/S0022-0000(03)00025-4 Special Issue on PODS 2001.

[4] Sören Auer, Christian Bizer, Georgi Kobilarov, Jens Lehmann, Richard Cyganiak, and Zachary Ives. 2007. DBpedia: a nucleus for a web of open data. In *Proceedings of the 6th International The Semantic Web and 2nd Asian Conference on Asian Semantic Web Conference* (Busan, Korea) *(ISWC'07/ASWC'07)*. Springer-Verlag, Berlin, Heidelberg, 722–735.

[5] Richard Baraniuk, Mark Davenport, Ronald DeVore, and Michael Wakin. 2008. A Simple Proof of the Restricted Isometry Property for Random Matrices. *Constructive Approximation* 28 (12 2008), 253–263. doi:10.1007/s00365-007-9003-x

[6] Yoav Benjamini and Yosef Hochberg. 1995. Controlling the False Discovery Rate: A Practical and Powerful Approach to Multiple Testing. *Journal of the Royal Statistical Society. Series B (Methodological)* 57, 1 (1995), 289–300. http://www.jstor.org/stable/2346101

[7] Antoine Bordes, Nicolas Usunier, Alberto Garcia-Durán, Jason Weston, and Oksana Yakhnenko. 2013. Translating embeddings for modeling multi-relational data. In *Proceedings of the 27th International Conference on Neural Information Processing Systems - Volume 2* (Lake Tahoe, Nevada) *(NIPS'13)*. Curran Associates Inc., Red Hook, NY, USA, 2787–2795.

[8] Emmanuel Candes, Justin Romberg, and Terence Tao. 2004. Robust Uncertainty Principles: Exact Signal Reconstruction from Highly Incomplete Frequency Information. arXiv:math/0409186 [math.NA] https://arxiv.org/abs/math/0409186

[9] Emmanuel Candès, Justin Romberg, and Terence Tao. 2006. Stable signal recovery from incomplete and inaccurate measurements. *Communications on Pure and Applied Mathematics* 59, 12 (2006), 1207–1223. https://onlinelibrary.wiley.com/doi/10.1002/cpa.20124

[10] Claudio Carpineto and Giovanni Romano. 2012. A Survey of Automatic Query Expansion in Information Retrieval. *ACM Comput. Surv.* 44, 1, Article 1 (Jan. 2012), 50 pages. doi:10.1145/2071389.2071390

[11] Kenneth Ward Church and Patrick Hanks. 1990. Word Association Norms, Mutual Information, and Lexicography. *Computational Linguistics* 16, 1 (1990), 22–29. https://aclanthology.org/J90-1003/

[12] Colin B. Clement, Matthew Bierbaum, Kevin P. O'Keeffe, and Alexander A. Alemi. 2019. On the Use of ArXiv as a Dataset. arXiv:1905.00075 [cs.IR] https://arxiv.org/abs/1905.00075

[13] Scott Deerwester, Susan T. Dumais, George W. Furnas, Thomas K. Landauer, and Richard Harshman. 1990. Indexing by latent semantic analysis. *Journal of the American Society for Information Science* 41, 6 (1990), 391–407. doi:10.1002/(SICI)1097-4571(199009)41:6<391::AID-ASI1>3.0.CO;2-9

[14] Jacob Devlin, Ming-Wei Chang, Kenton Lee, and Kristina Toutanova. 2019. BERT: Pre-training of Deep Bidirectional Transformers for Language Understanding. arXiv:1810.04805 [cs.CL] https://arxiv.org/abs/1810.04805

[15] Matthijs Douze, Alexandr Guzhva, Chengqi Deng, Jeff Johnson, Gergely Szilvasy, Pierre-Emmanuel Mazaré, Maria Lomeli, Lucas Hosseini, and Hervé Jégou. 2024. The Faiss library. (2024). arXiv:2401.08281 [cs.LG]

[16] Ahmed El-Kishky, Yanglei Song, Chi Wang, Clare R. Voss, and Jiawei Han. 2014. Scalable topical phrase mining from text corpora. *Proc. VLDB Endow.* 8, 3 (Nov. 2014), 305–316. doi:10.14778/2735508.2735519

[17] Usama M. Fayyad, Gregory Piatetsky-Shapiro, and Padhraic Smyth. 1996. *From data mining to knowledge discovery: an overview*. American Association for Artificial Intelligence, USA, 1–34.

[18] Simon Foucart and Holger Rauhut. 2013. *A Mathematical Introduction to Compressive Sensing*. Birkhäuser Basel.

[19] Cong Fu, Chao Xiang, Changxu Wang, and Deng Cai. 2019. Fast approximate nearest neighbor search with the navigating spreading-out graph. *Proc. VLDB Endow.* 12, 5 (Jan. 2019), 461–474. doi:10.14778/3303753.3303754

[20] Leslie Greengard and June-Yub Lee. 2004. Accelerating the Nonuniform Fast Fourier Transform. *SIAM Rev.* 46, 3 (2004), 443–454. arXiv:https://doi.org/10.1137/S003614450343200X doi:10.1137/S003614450343200X

[21] Nathan Halko, Per-Gunnar Martinsson, and Joel A. Tropp. 2010. Finding structure with randomness: Probabilistic algorithms for constructing approximate matrix decompositions. arXiv:0909.4061 [math.NA] https://arxiv.org/abs/0909.4061

[22] Aidan Hogan, Eva Blomqvist, Michael Cochez, Claudia D'amato, Gerard De Melo, Claudio Gutierrez, Sabrina Kirrane, José Emilio Labra Gayo, Roberto Navigli, Sebastian Neumaier, Axel-Cyrille Ngonga Ngomo, Axel Polleres, Sabbir M. Rashid, Anisa Rula, Lukas Schmelzeisen, Juan Sequeda, Steffen Staab, and Antoine Zimmermann. 2021. Knowledge Graphs. *Comput. Surveys* 54, 4 (July 2021), 1–37. doi:10.1145/3447772

[23] Ziwei Ji, Nayeon Lee, Rita Frieske, Tiezheng Yu, Dan Su, Yan Xu, Etsuko Ishii, Ye Jin Bang, Andrea Madotto, and Pascale Fung. 2023. Survey of Hallucination in Natural Language Generation. *Comput. Surveys* 55, 12 (March 2023), 1–38. doi:10.1145/3571730

[24] Jiawei Jiang, Fangcheng Fu, Tong Yang, and Bin Cui. 2018. SketchML: Accelerating Distributed Machine Learning with Data Sketches. In *Proceedings of the 2018 International Conference on Management of Data* (Houston, TX, USA) *(SIGMOD '18)*. Association for Computing Machinery, New York, NY, USA, 1269–1284. doi:10.1145/3183713.3196894

[25] Zhijing Jin, Qipeng Guo, Xipeng Qiu, and Zheng Zhang. 2020. GenWiki: A Dataset of 1.3 Million Content-Sharing Text and Graphs for Unsupervised Graph-to-Text Generation. In *Proceedings of the 28th International Conference on Computational Linguistics*, Donia Scott, Nuria Bel, and Chengqing Zong (Eds.). International Committee on Computational Linguistics, Barcelona, Spain (Online), 2398–2409. doi:10.18653/v1/2020.coling-main.217

[26] William B Johnson, Joram Lindenstrauss, et al. 1984. Extensions of Lipschitz mappings into a Hilbert space. *Contemporary mathematics* 26, 189-206 (1984), 1.

[27] Shantanu Kumar. 2017. A Survey of Deep Learning Methods for Relation Extraction. arXiv:1705.03645 [cs.CL] https://arxiv.org/abs/1705.03645

[28] Patrick Lewis, Ethan Perez, Aleksandra Piktus, Fabio Petroni, Vladimir Karpukhin, Naman Goyal, Heinrich Küttler, Mike Lewis, Wen-tau Yih, Tim Rocktäschel, Sebastian Riedel, and Douwe Kiela. 2020. Retrieval-augmented generation for knowledge-intensive NLP tasks. In *Proceedings of the 34th International Conference on Neural Information Processing Systems* (Vancouver, BC, Canada) *(NIPS '20)*. Curran Associates Inc., Red Hook, NY, USA, Article 793, 16 pages.

[29] Kejing Lu, Mineichi Kudo, Chuan Xiao, and Yoshiharu Ishikawa. 2021. HVS: hierarchical graph structure based on voronoi diagrams for solving approximate nearest neighbor search. *Proc. VLDB Endow.* 15, 2 (Oct. 2021), 246–258. doi:10.14778/3489496.3489506

[30] P. M. Mäkilä, J. R. Partington, and T. Norlander. 1998. Bounded Power Signal Spaces for Robust Control and Modeling. *SIAM Journal on Control and Optimization* 37, 1 (1998), 92–117. arXiv:https://doi.org/10.1137/S0363012997316664 doi:10.1137/S0363012997316664

[31] Yu A. Malkov and D. A. Yashunin. 2020. Efficient and Robust Approximate Nearest Neighbor Search Using Hierarchical Navigable Small World Graphs. *IEEE Trans. Pattern Anal. Mach. Intell.* 42, 4 (April 2020), 824–836. doi:10.1109/TPAMI.2018.2889473

[32] Christopher D Manning and Hinrich Schütze. 1999. Foundations of statistical natural language processing.

[33] Stefano Marchesin and Gianmaria Silvello. 2025. Credible Intervals for Knowledge Graph Accuracy Estimation. *Proc. ACM Manag. Data* 3, 3, Article 142 (June 2025), 26 pages. doi:10.1145/3725279

[34] Tomás Mikolov, Kai Chen, Greg Corrado, and Jeffrey Dean. 2013. Efficient Estimation of Word Representations in Vector Space. In *1st International Conference on Learning Representations, ICLR 2013, Scottsdale, Arizona, USA, May 2-4, 2013, Workshop Track Proceedings*. http://arxiv.org/abs/1301.3781

[35] Mike Mintz, Steven Bills, Rion Snow, and Daniel Jurafsky. 2009. Distant supervision for relation extraction without labeled data. In *Proceedings of the Joint Conference of the 47th Annual Meeting of the ACL and the 4th International Joint Conference on Natural Language Processing of the AFNLP*, Keh-Yih Su, Jian Su, Janyce Wiebe, and Haizhou Li (Eds.). Association for Computational Linguistics, Suntec, Singapore, 1003–1011. https://aclanthology.org/P09-1113/

[36] Maximilian Nickel, Volker Tresp, and Hans-Peter Kriegel. 2011. A three-way model for collective learning on multi-relational data. In *Proceedings of the 28th International Conference on International Conference on Machine Learning* (Bellevue, Washington, USA) *(ICML'11)*. Omnipress, Madison, WI, USA, 809–816.

[37] Reham Omar, Omij Mangukiya, and Essam Mansour. 2025. Dialogue Benchmark Generation from Knowledge Graphs with Cost-Effective Retrieval-Augmented LLMs. *Proc. ACM Manag. Data* 3, 1, Article 31 (Feb. 2025), 26 pages. doi:10.1145/3709681

[38] Shirui Pan, Linhao Luo, Yufei Wang, Chen Chen, Jiapu Wang, and Xindong Wu. 2024. Unifying Large Language Models and Knowledge Graphs: A Roadmap. *IEEE Transactions on Knowledge and Data Engineering* 36, 7 (July 2024), 3580–3599. doi:10.1109/tkde.2024.3352100

[39] Jeffrey Pennington, Richard Socher, and Christopher Manning. 2014. GloVe: Global Vectors for Word Representation. In *Proceedings of the 2014 Conference on Empirical Methods in Natural Language Processing (EMNLP)*, Alessandro Moschitti, Bo Pang, and Walter Daelemans (Eds.). Association for Computational Linguistics, Doha, Qatar, 1532–1543. doi:10.3115/v1/D14-1162

[40] Ali Rahimi and Benjamin Recht. 2007. Random Features for Large-Scale Kernel Machines. In *Advances in Neural Information Processing Systems*, J. Platt, D. Koller, Y. Singer, and S. Roweis (Eds.), Vol. 20. Curran Associates, Inc. https://proceedings.neurips.cc/paper_files/paper/2007/file/013a006f03dbc5392effeb8f18fda755-Paper.pdf

[41] Diego Rincon-Yanez and Sabrina Senatore. 2022. FAIR Knowledge Graph construction from text, an approach applied to fictional novels. In *Proceedings of the 1st International Workshop on Knowledge Graph Generation From Text and*

the 1st International Workshop on Modular Knowledge co-located with 19th Extended Semantic Conference (ESWC 2022). CEUR-WS, Hersonissos, Greece, 94–108. http://ceur-ws.org/Vol-3184/TEXT2KG_Paper_7.pdf

[42] Stephen Robertson and Hugo Zaragoza. 2009. The Probabilistic Relevance Framework: BM25 and Beyond. *Found. Trends Inf. Retr.* 3, 4 (April 2009), 333–389. doi:10.1561/1500000019

[43] Florin Rusu and Alin Dobra. 2007. Statistical analysis of sketch estimators. In *Proceedings of the 2007 ACM SIGMOD International Conference on Management of Data* (Beijing, China) *(SIGMOD '07).* Association for Computing Machinery, New York, NY, USA, 187–198. doi:10.1145/1247480.1247503

[44] Chuan Shi, Yitong Li, Jiawei Zhang, Yizhou Sun, and Philip S. Yu. 2017. A Survey of Heterogeneous Information Network Analysis. *IEEE Trans. on Knowl. and Data Eng.* 29, 1 (Jan. 2017), 17–37. doi:10.1109/TKDE.2016.2598561

[45] Joel A. Tropp and Anna C. Gilbert. 2007. Signal Recovery From Random Measurements Via Orthogonal Matching Pursuit. *IEEE Transactions on Information Theory* 53, 12 (2007), 4655–4666. doi:10.1109/TIT.2007.909108

[46] Stephan Tulkens and Thomas van Dongen. 2024. *Model2Vec: Fast State-of-the-Art Static Embeddings.* doi:10.5281/zenodo.17270888

[47] Feiyu Wang, Qizhi Chen, Yuanpeng Li, Tong Yang, Yaofeng Tu, Lian Yu, and Bin Cui. 2023. JoinSketch: A Sketch Algorithm for Accurate and Unbiased Inner-Product Estimation. *Proc. ACM Manag. Data* 1, 1, Article 81 (May 2023), 26 pages. doi:10.1145/3588935

[48] Mengzhao Wang, Xiaoliang Xu, Qiang Yue, and Yuxiang Wang. 2021. A comprehensive survey and experimental comparison of graph-based approximate nearest neighbor search. *Proc. VLDB Endow.* 14, 11 (July 2021), 1964–1978. doi:10.14778/3476249.3476255

[49] Hao Yan, Shuming Shi, Fan Zhang, Torsten Suel, and Ji-Rong Wen. 2010. Efficient term proximity search with term-pair indexes. In *Proceedings of the 19th ACM International Conference on Information and Knowledge Management* (Toronto, ON, Canada) *(CIKM '10).* Association for Computing Machinery, New York, NY, USA, 1229–1238. doi:10.1145/1871437.1871593

[50] Huiyuan Yu, Jia He, and Maggie Cheng. 2025. Fast Orthogonal Matching Pursuit through Successive Regression. arXiv:2404.00146 [cs.CV] https://arxiv.org/abs/2404.00146

[51] Xi Zhao, Yao Tian, Kai Huang, Bolong Zheng, and Xiaofang Zhou. 2023. Towards Efficient Index Construction and Approximate Nearest Neighbor Search in High-Dimensional Spaces. *Proc. VLDB Endow.* 16, 8 (April 2023), 1979–1991. doi:10.14778/3594512.3594527

Appendix: Detailed Proofs of Theorems

This appendix provides comprehensive and detailed proofs for the key theorems stated in Section 3, ensuring mathematical rigor and completeness.

Proof of Theorem 3.1: Inner Product Preservation

We restate Theorem 3.1 for clarity.

THEOREM (THEOREM 3.1: INNER PRODUCT PRESERVATION). *For any two term vectors $\tilde{\mathbf{a}}_i, \tilde{\mathbf{a}}_j \in \mathbb{R}^M$, their randomized Fourier embeddings $\mathbf{b}_i, \mathbf{b}_j \in \mathbb{C}^k$, defined by $\mathbf{b}_i = \frac{1}{\sqrt{k}}\boldsymbol{\Phi}\tilde{\mathbf{a}}_i$ where $\phi_{lm} = e^{-2\pi i \xi_l m/M}$ and $\xi_l \sim Uniform(0,1)$, satisfy:*

(1) $\mathbb{E}[\langle \mathbf{b}_i, \mathbf{b}_j \rangle] = \langle \tilde{\mathbf{a}}_i, \tilde{\mathbf{a}}_j \rangle$
(2) $\mathrm{Var}(\langle \mathbf{b}_i, \mathbf{b}_j \rangle) = \frac{1}{k}\left(\|\tilde{\mathbf{a}}_i\|^2 \|\tilde{\mathbf{a}}_j\|^2 - 2\sum_{m=1}^M \tilde{a}_{im}^2 \tilde{a}_{jm}^2 \right)$

PROOF. Let $X = \langle \mathbf{b}_i, \mathbf{b}_j \rangle = \mathbf{b}_j^* \mathbf{b}_i = \sum_{l=1}^k \overline{b_{j,l}}\, b_{i,l}$.

Part 1: Expectation. We begin by analyzing a single component l of the sum. By definition:

$$b_{i,l} = \frac{1}{\sqrt{k}}\sum_{m=1}^M \phi_{lm}\tilde{a}_{im} = \frac{1}{\sqrt{k}}\sum_{m=1}^M e^{-2\pi i \xi_l m/M}\tilde{a}_{im},$$

$$\overline{b_{j,l}} = \frac{1}{\sqrt{k}}\sum_{n=1}^M \overline{\phi_{ln}}\,\tilde{a}_{jn} = \frac{1}{\sqrt{k}}\sum_{n=1}^M e^{2\pi i \xi_l n/M}\tilde{a}_{jn}.$$

Their product is:

$$\overline{b_{j,l}}\, b_{i,l} = \frac{1}{k}\sum_{m=1}^M \sum_{n=1}^M e^{-2\pi i \xi_l (m-n)/M}\tilde{a}_{im}\tilde{a}_{jn}.$$

Taking the expectation with respect to the random variable ξ_l:

$$\mathbb{E}_{\xi_l}[\overline{b_{j,l}}\, b_{i,l}] = \frac{1}{k}\sum_{m=1}^M \sum_{n=1}^M \tilde{a}_{im}\tilde{a}_{jn}\,\mathbb{E}_{\xi_l}\left[e^{-2\pi i \xi_l (m-n)/M} \right]$$

$$= \frac{1}{k}\sum_{m=1}^M \sum_{n=1}^M \tilde{a}_{im}\tilde{a}_{jn}\int_0^1 e^{-2\pi i t(m-n)/M}dt.$$

The value of the integral is:

$$\int_0^1 e^{-2\pi i t(m-n)/M}dt = \begin{cases} 1 & \text{if } m = n, \\ 0 & \text{if } m \neq n. \end{cases}$$

Thus, the double sum collapses to the case $m = n$:

$$\mathbb{E}_{\xi_l}[\overline{b_{j,l}}\, b_{i,l}] = \frac{1}{k}\sum_{m=1}^M \tilde{a}_{im}\tilde{a}_{jm} = \frac{1}{k}\langle \tilde{\mathbf{a}}_i, \tilde{\mathbf{a}}_j \rangle.$$

Since the ξ_l for $l = 1, \ldots, k$ are independent and identically distributed (i.i.d.), the expectation of the full inner product is:

$$\mathbb{E}[X] = \mathbb{E}\left[\sum_{l=1}^k \overline{b_{j,l}}\, b_{i,l} \right]$$

$$= \sum_{l=1}^k \mathbb{E}_{\xi_l}[\overline{b_{j,l}}\, b_{i,l}]$$

$$= \sum_{l=1}^k \frac{1}{k}\langle \tilde{\mathbf{a}}_i, \tilde{\mathbf{a}}_j \rangle = \langle \tilde{\mathbf{a}}_i, \tilde{\mathbf{a}}_j \rangle.$$

This proves the first statement.

Part 2: Variance. The variance of the complex random variable X is defined as $\mathrm{Var}(X) = \mathbb{E}[|X|^2] - |\mathbb{E}[X]|^2$. We already have $|\mathbb{E}[X]|^2 = |\langle \tilde{\mathbf{a}}_i, \tilde{\mathbf{a}}_j \rangle|^2$.

We now compute $\mathbb{E}[|X|^2]$:

$$\mathbb{E}[|X|^2] = \sum_{l=1}^k \sum_{l'=1}^k \mathbb{E}\left[\overline{b_{j,l}}\, b_{i,l}\, b_{j,l'}\, \overline{b_{i,l'}} \right].$$

We analyze this double sum by considering the cases where $l = l'$ and $l \neq l'$.

Case 1: $l = l'$. (k terms). The contribution from these terms is:

$$S_1 = k \cdot \mathbb{E}_{\xi_l}\left[|b_{i,l}|^2 |b_{j,l}|^2 \right]$$

$$= \frac{1}{k}\left(\|\tilde{\mathbf{a}}_i\|^2 \|\tilde{\mathbf{a}}_j\|^2 + |\langle \tilde{\mathbf{a}}_i, \tilde{\mathbf{a}}_j \rangle|^2 - 2\sum_{m=1}^M \tilde{a}_{im}^2 \tilde{a}_{jm}^2 \right).$$

Case 2: $l \neq l'$. ($k(k-1)$ terms). By independence of ξ_l and $\xi_{l'}$, the contribution is:

$$S_2 = k(k-1) \cdot \mathbb{E}\left[\overline{b_{j,l}}b_{i,l} \right] \mathbb{E}\left[b_{j,l'}\overline{b_{i,l'}} \right] = \frac{k-1}{k}|\langle \tilde{\mathbf{a}}_i, \tilde{\mathbf{a}}_j \rangle|^2.$$

Combining the contributions:

$$\mathbb{E}[|X|^2] = S_1 + S_2$$

$$= \frac{1}{k}\left(\|\tilde{\mathbf{a}}_i\|^2 \|\tilde{\mathbf{a}}_j\|^2 + |\langle \tilde{\mathbf{a}}_i, \tilde{\mathbf{a}}_j \rangle|^2 - 2\sum_{m=1}^M \tilde{a}_{im}^2 \tilde{a}_{jm}^2 \right)$$

$$+ \frac{k-1}{k}|\langle \tilde{\mathbf{a}}_i, \tilde{\mathbf{a}}_j \rangle|^2$$

$$= \frac{1}{k}\|\tilde{\mathbf{a}}_i\|^2 \|\tilde{\mathbf{a}}_j\|^2 + |\langle \tilde{\mathbf{a}}_i, \tilde{\mathbf{a}}_j \rangle|^2 - \frac{2}{k}\sum_{m=1}^M \tilde{a}_{im}^2 \tilde{a}_{jm}^2.$$

Finally, we obtain the variance:

$$\mathrm{Var}(X) = \mathbb{E}[|X|^2] - |\mathbb{E}[X]|^2$$

$$= \frac{1}{k}\|\tilde{\mathbf{a}}_i\|^2 \|\tilde{\mathbf{a}}_j\|^2 + |\langle \tilde{\mathbf{a}}_i, \tilde{\mathbf{a}}_j \rangle|^2$$

$$- \frac{2}{k}\sum_{m=1}^M \tilde{a}_{im}^2 \tilde{a}_{jm}^2 - |\langle \tilde{\mathbf{a}}_i, \tilde{\mathbf{a}}_j \rangle|^2$$

$$= \frac{1}{k}\left(\|\tilde{\mathbf{a}}_i\|^2 \|\tilde{\mathbf{a}}_j\|^2 - 2\sum_{m=1}^M \tilde{a}_{im}^2 \tilde{a}_{jm}^2 \right).$$

This proves the second statement. □

Proof of Theorem 3.2: CPSD Correlation Estimator

THEOREM (THEOREM 3.2: CPSD CORRELATION ESTIMATOR). *The normalized real part of the CPSD provides a consistent estimator for the Pearson correlation:*

$$\hat{\rho}_{ij} = \frac{\Re(P_{ij})}{\sqrt{P_{ii}}\sqrt{P_{jj}}} \xrightarrow{p} \rho_{ij} \quad as \quad k \to \infty.$$

PROOF. Let $U_k = \Re(P_{ij})$, $V_k = P_{ii}$, and $W_k = P_{jj}$. Our estimator is a function of these variables, $\hat{\rho}_{ij} = g(U_k, V_k, W_k) = U_k/(\sqrt{V_k}\sqrt{W_k})$.

From Theorem 3.1, we have $\mathbb{E}[P_{ij}] = \langle \tilde{\mathbf{a}}_i, \tilde{\mathbf{a}}_j \rangle$ and $\mathrm{Var}(P_{ij}) = O(1/k)$. By Chebyshev's inequality, this implies that P_{ij} converges

in probability to its mean, $P_{ij} \xrightarrow{p} \langle \tilde{\mathbf{a}}_i, \tilde{\mathbf{a}}_j \rangle$. The same holds for the diagonal terms, $P_{ii} \xrightarrow{p} \|\tilde{\mathbf{a}}_i\|^2$ and $P_{jj} \xrightarrow{p} \|\tilde{\mathbf{a}}_j\|^2$.

The function $g(u, v, w)$ is continuous for $v > 0, w > 0$, and the functions $\Re(\cdot)$ and $\sqrt{\cdot}$ are also continuous. By the continuous mapping theorem, the sequence of random vectors (U_k, V_k, W_k) converges in probability to the constant vector $(\langle \tilde{\mathbf{a}}_i, \tilde{\mathbf{a}}_j \rangle, \|\tilde{\mathbf{a}}_i\|^2, \|\tilde{\mathbf{a}}_j\|^2)$. Applying the continuous function g to this sequence, we get:

$$\hat{\rho}_{ij} = g(U_k, V_k, W_k) \xrightarrow{p} g(\langle \tilde{\mathbf{a}}_i, \tilde{\mathbf{a}}_j \rangle, \|\tilde{\mathbf{a}}_i\|^2, \|\tilde{\mathbf{a}}_j\|^2) = \frac{\langle \tilde{\mathbf{a}}_i, \tilde{\mathbf{a}}_j \rangle}{\|\tilde{\mathbf{a}}_i\| \|\tilde{\mathbf{a}}_j\|} = \rho_{ij}.$$

This proves that $\hat{\rho}_{ij}$ is a consistent estimator for ρ_{ij}. $\qquad \square$

Proof of Lemma 3.3 Error Bound for Correlation Estimation

PROOF. The proof proceeds in three steps: bounding the error in the numerator, bounding the error in the denominators, and then combining them via a Taylor expansion and concentration inequalities.

Step 1: Bounding the Numerator. Let $X_l = \Re(\langle \mathbf{z}_l, \tilde{\mathbf{a}}_i \rangle \langle \mathbf{z}_l, \tilde{\mathbf{a}}_j \rangle)$ for $l = 1, \ldots, k$, where $\mathbf{z}_l$ is the l-th row of Φ. From the construction of the embedding, we have:

$$\Re(P_{ij}) = \frac{1}{k} \sum_{l=1}^{k} X_l$$

From Theorem 3.1, we know $\mathbb{E}[X_l] = \tilde{\mathbf{a}}_i^\top \tilde{\mathbf{a}}_j$ and $\mathrm{Var}(X_l) \leq \sigma^2$ for some fixed σ^2 (which depends on $\|\tilde{\mathbf{a}}_i\|$ and $\|\tilde{\mathbf{a}}_j\|$ but not on k). Furthermore, since the $\mathbf{z}_l$ are bounded, the X_l are sub-Gaussian random variables. Applying a Hoeffding-type inequality for sub-Gaussian random variables, we get:

$$\mathbb{P}\left(\left| \Re(P_{ij}) - \tilde{\mathbf{a}}_i^\top \tilde{\mathbf{a}}_j \right| \geq t \right) \leq 2 \exp\left(-\frac{ckt^2}{\sigma^2} \right) \qquad (17)$$

for some constant $c > 0$.

Step 2: Bounding the Denominators. Similarly, consider the variance estimates. Let $Y_l = |\langle \mathbf{z}_l, \tilde{\mathbf{a}}_i \rangle|^2$. Then $P_{ii} = \frac{1}{k} \sum_{l=1}^{k} Y_l$, with $\mathbb{E}[Y_l] = \|\tilde{\mathbf{a}}_i\|^2$ and $\mathrm{Var}(Y_l) \leq \gamma_i^2$. Again, by sub-Gaussian concentration:

$$\mathbb{P}\left(\left| P_{ii} - \|\tilde{\mathbf{a}}_i\|^2 \right| \geq t \right) \leq 2 \exp\left(-\frac{ckt^2}{\gamma_i^2} \right) \qquad (18)$$

To bound the error of the square root, we use the fact that the function $f(x) = \sqrt{x}$ is Lipschitz continuous for $x \geq \eta > 0$ (which holds since we assume non-zero vectors). Let $L = 1/(2\sqrt{\eta})$ be the Lipschitz constant. From (18) and the Lipschitz property, we derive:

$$\mathbb{P}\left(\left| \sqrt{P_{ii}} - \|\tilde{\mathbf{a}}_i\| \right| \geq t \right) \leq 2 \exp\left(-\frac{ckt^2}{L^2 \gamma_i^2} \right) \qquad (19)$$

An identical bound holds for $\sqrt{P_{jj}}$.

Step 3: Combining the Errors via Taylor Expansion. The estimator is a function of three random variables:

$$\hat{\rho}_{ij} = f(U, V, W) = \frac{U}{\sqrt{V} \sqrt{W}}$$

where $U = \Re(P_{ij})$, $V = P_{ii}$, $W = P_{jj}$. We perform a first-order Taylor expansion around the true values $u_0 = \tilde{\mathbf{a}}_i^\top \tilde{\mathbf{a}}_j$, $v_0 = \|\tilde{\mathbf{a}}_i\|^2$,

$w_0 = \|\tilde{\mathbf{a}}_j\|^2$:

$$f(U, V, W) - f(u_0, v_0, w_0) \approx \frac{\partial f}{\partial U}\bigg|_0 (U - u_0) +$$
$$\frac{\partial f}{\partial V}\bigg|_0 (V - v_0) +$$
$$\frac{\partial f}{\partial W}\bigg|_0 (W - w_0) = \frac{1}{\|\tilde{\mathbf{a}}_i\| \|\tilde{\mathbf{a}}_j\|} (U - u_0)$$
$$- \frac{\tilde{\mathbf{a}}_i^\top \tilde{\mathbf{a}}_j}{2\|\tilde{\mathbf{a}}_i\|^3 \|\tilde{\mathbf{a}}_j\|} (V - v_0) - \frac{\tilde{\mathbf{a}}_i^\top \tilde{\mathbf{a}}_j}{2\|\tilde{\mathbf{a}}_i\| \|\tilde{\mathbf{a}}_j\|^3} (W - w_0)$$

The error $|\hat{\rho}_{ij} - \rho_{ij}|$ is therefore bounded by a linear combination of $|U - u_0|$, $|V - v_0|$, and $|W - w_0|$. Since U, V, and W are independent (as they are constructed from independent random features), we can combine the concentration bounds (17) and (19) via a union bound.

Setting $t = \epsilon$ in each of the three bounds and applying the union bound yields:

$$\mathbb{P}\left(|\hat{\rho}_{ij} - \rho_{ij}| \geq C_1 \epsilon \right) \leq 6 \exp\left(-\frac{ck\epsilon^2}{\max(\sigma^2, L^2 \gamma_i^2, L^2 \gamma_j^2)} \right)$$

for a new constant C_1. Let $\delta = 6 \exp\left(-\frac{ck\epsilon^2}{C_2} \right)$, where $C_2 = \max(\sigma^2, L^2 \gamma_i^2, L^2 \gamma_j^2)$. Solving for ϵ gives $\epsilon = \sqrt{\frac{C_2}{ck} \log(6/\delta)}$. Substituting back, we conclude that with probability at least $1 - \delta$,

$$|\hat{\rho}_{ij} - \rho_{ij}| \leq C\sqrt{\frac{\log(1/\delta)}{k}}$$

where the constant C absorbs C_1, C_2, c, and the $\log(6)$ factor. $\quad \square$

Justification for Theorem 4.1: OMP Sparse Recovery Guarantee

THEOREM (THEOREM 4.1: OMP RECOVERY GUARANTEE). *If the sensing matrix Ψ satisfies the Restricted Isometry Property (RIP) of order $S + 1$ with a sufficiently small constant δ_{S+1}, then the solution $\hat{\mathbf{x}}_i$ produced by the Orthogonal Matching Pursuit (OMP) algorithm after S steps from the measurement model $\mathbf{z}_i = \Psi \rho_i + \mathbf{e}$ satisfies:*

$$\|\hat{\mathbf{x}}_i - \rho_i\|_2 \leq C_1 \|\mathbf{e}\|_2 + C_2 \frac{\|\rho_i - \rho_i^S\|_1}{\sqrt{S}},$$

where $\mathbf{e}$ is the noise vector, ρ_i^S is the best S-term approximation of ρ_i, and C_1, C_2 are constants.

JUSTIFICATION. This theorem is an application of a foundational result in compressed sensing, by Candès et. al., [9]. The guarantee for the OMP algorithm relies on two key properties of the compressed sensing framework:

1. **RIP of the Sensing Matrix Ψ**: The matrix Ψ is constructed by normalizing the columns of the embedding matrix $\mathbf{B}$ (i.e., $\psi_j = \mathbf{b}_j / \|\mathbf{b}_j\|$). It is a well-established property that random matrices, including those constructed from orthonormal systems like the Fourier system, satisfy the RIP with high probability. This property ensures that Ψ approximately preserves the lengths of all sparse vectors, which is the crucial geometric condition that allows greedy algorithms like OMP to succeed. For the RIP to hold, the number of measurements k must be sufficiently large relative to the sparsity level S, typically on the order of $k \gtrsim S \log(N/S)$.

2. **Stable Recovery Guarantee for OMP**: When the sensing matrix Ψ satisfies the RIP, the greedy nature of the OMP algorithm is guaranteed to provide a stable and robust recovery of the underlying signal ρ_i. The algorithm works by iteratively identifying the column of Ψ most correlated with the current residual and projecting the measurement onto the space spanned by the selected columns. The error bound reflects the algorithm's robustness to both noise and signals that are not perfectly sparse:

- **Noise Term** ($C_1 \|\mathbf{e}\|_2$): This term bounds the error's dependence on the energy of the measurement noise $\mathbf{e}$. In our case, this noise arises from the approximation error inherent in the random Fourier embedding.

- **Approximation Term** ($C_2 \frac{\|\rho_i - \rho_i^S\|_1}{\sqrt{S}}$): This term accounts for the fact that the true correlation vector ρ_i may not be perfectly sparse, but only *compressible* (i.e., its sorted coefficients decay rapidly). The recovery error degrades gracefully with how well the signal can be approximated by its largest S components.

The constants C_1, C_2 depend only on the RIP constant δ_{S+1}. By ensuring our embedding dimension k is sufficiently large, we meet the conditions for this theorem, enabling reliable recovery of the significant correlations for each term via the computationally efficient OMP algorithm. $\square$